Published for SISSA by Springer

Received: June 12, 2017
Revised: September 27, 2017
Accepted: October 6, 2017
Published: November 15, 2017

Measurement of the $t\bar{t}\gamma$ production cross section in proton-proton collisions at $\sqrt{s} = 8$ TeV with the ATLAS detector

The ATLAS collaboration

E-mail: atlas.publications@cern.ch

Abstract: The cross section of a top-quark pair produced in association with a photon is measured in proton-proton collisions at a centre-of-mass energy of $\sqrt{s} = 8$ TeV with $20.2\,\text{fb}^{-1}$ of data collected by the ATLAS detector at the Large Hadron Collider in 2012. The measurement is performed by selecting events that contain a photon with transverse momentum $p_{\text{T}} > 15$ GeV, an isolated lepton with large transverse momentum, large missing transverse momentum, and at least four jets, where at least one is identified as originating from a b-quark. The production cross section is measured in a fiducial region close to the selection requirements. It is found to be $139 \pm 7\,(\text{stat.}) \pm 17\,(\text{syst.})$ fb, in good agreement with the theoretical prediction at next-to-leading order of 151 ± 24 fb. In addition, differential cross sections in the fiducial region are measured as a function of the transverse momentum and pseudorapidity of the photon.

Keywords: Hadron-Hadron scattering (experiments), Top physics

ArXiv ePrint: 1706.03046

Open Access, Copyright CERN,
for the benefit of the ATLAS Collaboration.
Article funded by SCOAP[3].

https://doi.org/10.1007/JHEP11(2017)086

JHEP11(2017)086

source: https://doi.org/10.7892/boris.114251 | downloaded: 12.10.2024

Contents

1 Introduction **1**

2 ATLAS detector **1**

3 Data and simulation samples **2**

4 Event reconstruction and selection **3**
- 4.1 Event reconstruction 3
- 4.2 Event selection 5
- 4.3 Definition of the fiducial phase space 6

5 Templates **8**
- 5.1 Prompt-photon template 8
- 5.2 Hadronic-fake template 8
- 5.3 Electron-fake template 10

6 Background estimation **10**
- 6.1 Background from hadrons misidentified as photons 10
- 6.2 Background from electrons misidentified as photons 10
- 6.3 Background events with a prompt photon 11

7 Measurement of the fiducial cross section **12**
- 7.1 Theoretical prediction 12
- 7.2 Fit strategy 13

8 Systematic uncertainties **14**
- 8.1 Modelling uncertainties 15
- 8.2 Experimental uncertainties 15
- 8.3 Template-related uncertainties 16

9 Results **16**

10 Conclusions **18**

The ATLAS collaboration **25**

JHEP11(2017)086

1 Introduction

Measurements of top-quark properties play an important role in testing the Standard Model (SM) and its possible extensions. Studies of the production and dynamics of a top-quark pair in association with a photon ($t\bar{t}\gamma$) probe the $t\gamma$ electroweak coupling. For instance, deviations in the p_{T} spectrum of the photon from the SM prediction could point to new physics through anomalous dipole moments of the top quark, as discussed in refs. [1–6].

Photons can originate not only from top quarks, but also from their decay products, including the quarks and leptons from the decay of the W bosons. In addition, they can be radiated from incoming partons. Evidence for the production of a top-quark pair in association with an energetic, isolated photon has been found in $p\bar{p}$ collisions at the Tevatron collider at a centre-of-mass energy of $\sqrt{s} = 1.96\,\mathrm{TeV}$ by the CDF Collaboration [7]. Finally, observation of the $t\bar{t}\gamma$ process was reported by the ATLAS Collaboration in pp collisions at $\sqrt{s} = 7\,\mathrm{TeV}$ [8].

This paper describes a measurement of the $t\bar{t}\gamma$ production cross section, based on a data set recorded with the ATLAS detector in 2012 at a centre-of-mass energy of $\sqrt{s} = 8\,\mathrm{TeV}$ and corresponding to an integrated luminosity of $20.2\,\mathrm{fb}^{-1}$. The cross section is measured with a maximum-likelihood fit using templates defined within a fiducial volume chosen to be close to the selection requirements implemented in the analysis. Only final states with exactly one reconstructed lepton (electron or muon), including those originating from τ lepton decays, are considered. These final states are referred to as the single-lepton channel in the following. In addition to the inclusive cross section, differential cross sections as a function of the transverse momentum p_{T} and the pseudorapidity η of the photon are measured for the same fiducial volume. The cross sections are compared to the theoretical calculations at next-to-leading order (NLO) [9] in the strong interaction.

2 ATLAS detector

The ATLAS detector is described in detail elsewhere [10]. Here, a short overview is presented with a focus on the electromagnetic calorimeter, which provides an accurate measurement of energetic photons. The major components of the ATLAS detector are an inner detector (ID) surrounded by a thin superconducting solenoid providing a 2 T axial magnetic field, electromagnetic (EM) and hadronic calorimeters, and a muon spectrometer (MS). The ID provides tracking information and is composed of three subsystems. The pixel and silicon microstrip detectors cover the pseudorapidity range $|\eta| < 2.5$,[1] while the transition radiation tracker has an acceptance range of $|\eta| < 2.0$ and provides identification information for electrons. The MS consists of a large superconducting air-core toroidal magnet system, three stations of chambers for high-precision tracking measurements in the region $|\eta| < 2.7$, and a muon trigger system effective over the region $|\eta| < 2.4$.

[1] ATLAS uses a right-handed coordinate system with its origin at the nominal interaction point (IP) in the centre of the detector and the z-axis along the beam pipe. The x-axis points from the IP to the centre of the LHC ring, and the y-axis points upward. Cylindrical coordinates (r, ϕ) are used in the transverse plane, ϕ being the azimuthal angle around the z-axis. The pseudorapidity is defined in terms of the polar angle θ as $\eta = -\ln\tan(\theta/2)$.

JHEP11(2017)086

The electromagnetic calorimeter (EMC) is a lead/liquid-argon detector composed of a barrel ($|\eta| < 1.475$) and two endcaps ($1.375 < |\eta| < 3.2$). For $|\eta| < 2.5$, the calorimeter has three layers, longitudinal in shower depth, with the first layer having the highest granularity in the η direction, and the second layer collecting most of the electromagnetic shower energy for high-p_{T} electrons or photons. A thin presampling layer in the range $|\eta| < 1.8$ is used to correct for the energy lost by EM particles upstream of the calorimeter. The hadronic calorimeter system, which surrounds the electromagnetic calorimeter, is based on two different active media, scintillator tiles or liquid argon, and with steel, copper, or tungsten as the absorber materials. Photons are identified as narrow, isolated showers in the EMC with no spill-over into the hadronic calorimeter. The fine segmentation of the ATLAS calorimeter allows efficient rejection of jets fragmenting to high-energy π^0 or η mesons that could be misidentified as isolated prompt photons.

3 Data and simulation samples

Monte Carlo simulated events are used to evaluate signal efficiencies and backgrounds, and to estimate and correct for resolution effects. Additional simulated inelastic pp collisions, generated with Pythia 8.160 [11] using the `MSTW2008` LO [12] parton distribution functions (PDFs) and parameter values set according to the `A2` tune [13], are overlaid to simulate the effects of pile-up from additional interactions in the same and nearby bunch crossings.

The $t\bar{t}\gamma$ signal sample is modelled with MadGraph5_aMC@NLO 2.1.0 [14], interfaced to Pythia 6.427 [15] for parton showering and hadronisation. The $t\bar{t}\gamma$ matrix element is generated at leading order (LO) including the decays of the top quarks. The photons can be emitted from the incoming partons, from the top quark, or from the decay products. The renormalisation (μ_{R}) and factorisation (μ_{F}) scales are chosen such that the top-quark pair ($t\bar{t}$) events, produced with the same settings as used for the $t\bar{t}\gamma$ production, describe the $t\bar{t}$ data well. The scale choice is made to have the best agreement with the results in ref. [16]. Good agreement with the data is obtained for $\mu_{\mathrm{R}} = \mu_{\mathrm{F}} = 2m_{\mathrm{top}}$, where $m_{\mathrm{top}} = 172.5\,\mathrm{GeV}$ is the mass of the top quark used in all simulated samples. In order to avoid infrared and collinear singularities, the following kinematic requirements are applied to the generated events: the photon transverse momentum must be larger than 10 GeV and the absolute value of its pseudorapidity less than 5, at least one charged lepton with a transverse momentum larger than 15 GeV, and the distance $\Delta R = \sqrt{(\Delta\eta)^2 + (\Delta\phi)^2}$ between the photon and all other charged particles in the final state must be larger than 0.2. The `CTEQ6L1` (LO) PDF [17] is used both for the matrix element and in the Pythia 6 parton shower, using the corresponding `Perugia2011C` tune [18]. Additional photon radiation is generated with Photos 2.15.4 [19, 20]. The decays of the τ leptons are handled by Tauola 2.7 [21]. The signal sample is simulated for single-lepton and dilepton $t\bar{t}\gamma$ events. The sample is normalised to the NLO prediction using K-factors, as described in section 7.2.

The production of $W\gamma$+jets and $Z\gamma$+jets final states is simulated with the Sherpa 1.4.0 [22] event generator, using the NLO `CT10` PDF [23]. The matrix elements are calculated at LO with up to three final-state partons. The parton shower uses Sherpa's default set of tuned parameters. To evaluate the uncertainty due to $W\gamma$+jets modelling, an

JHEP11(2017)086

additional sample generated with Alpgen 2.14 [24], interfaced to Pythia 6.426, is used. For both the matrix-element calculations and the parton-shower evolution, the CTEQ6L1 PDF is used. The tuned parameters for the parton shower, the additional photon radiation, and τ lepton decays are handled in the same way as for the signal $t\bar{t}\gamma$ sample. No dedicated samples were produced for $Z\gamma$+jets final states due to the expected small contribution to the total uncertainty.

Electroweak production of the top quark (single-top) is simulated with Powheg-Box v1.0 [25, 26] using the NLO CT10 PDF. The same models are employed for parton shower, photon radiation, and τ lepton decays as used for the signal $t\bar{t}\gamma$ sample. The event generator versions for these processes are the ones used for the $t\bar{t}\gamma$ sample, apart from Pythia 6.426 being used for the showering of the Wt channel. In order to remove the overlap with $t\bar{t}$, the Wt sample is produced using the so-called diagram removal generation scheme [27]. The t-channel and Wt-channel samples are normalised to the approximate next-to-next-to-leading order calculations in refs. [28] and [29], respectively. In addition, diboson (WW, WZ, ZZ) production samples are generated using Alpgen 2.14 [24], interfaced to Herwig 6.520 [30] and Jimmy 4.31 [31]. For these, the CTEQ6L1 PDF and the corresponding AUET2 tune [32] are used. The additional photon radiation and τ lepton decays are handled in the same way as for the signal $t\bar{t}\gamma$ sample. The samples are normalised using the NLO calculation in ref. [33].

The $t\bar{t}$ process is simulated using the NLO quantum-chromodynamics (QCD) matrix-element event generator Powheg-Box v1.0 [34–36], using the CT10 PDF and interfaced to Pythia 6.427 for the parton shower, fragmentation and underlying-event modelling. Other settings are handled in the same way as for the signal $t\bar{t}\gamma$ sample. This sample is used exclusively to validate the data-driven backgrounds.

All samples are processed either through the full ATLAS detector simulation [37] based on Geant 4 [38], or through a faster simulation using parameterised showers in the calorimeters [39]. The resulting simulated events are processed with the same reconstruction algorithms and analysis chain as the data.

The measurement is based on data collected by the ATLAS experiment in pp collisions at $\sqrt{s} = 8$ TeV in 2012. The corresponding integrated luminosity is $20.2\,\text{fb}^{-1}$. The absolute luminosity scale is derived from beam-separation scans performed in November 2012 [40].

4 Event reconstruction and selection

The single-lepton $t\bar{t}\gamma$ final state is characterised by the presence of a high-p_{T} photon, an isolated lepton with a large p_{T}, large missing transverse momentum originating from the neutrino in the leptonic decay of a W boson, two jets from the hadronic decay of the other W boson, and two b-quark jets.

4.1 Event reconstruction

Electron candidates are reconstructed from energy deposits in the central region of the EMC with associated tracks in the ID [41]. The candidates have to satisfy the tight identification criteria [42] and are required to have a transverse momentum of $p_{\text{T}} > 25$ GeV and

JHEP11(2017)086

$|\eta_{\rm cl}| < 2.47$, excluding the transition region between barrel and endcap EM calorimeters, $1.37 < |\eta_{\rm cl}| < 1.52$. The variable $\eta_{\rm cl}$ is the pseudorapidity of the electromagnetic energy cluster with respect to the geometric centre of the detector. Electrons are further required to have a longitudinal impact parameter with respect to the primary vertex[2] of less than 2 mm. Isolation requirements on calorimeter and tracking variables are used to reduce the background from jets misidentified as electrons. The calorimeter isolation variable is based on the energy sum of cells within a cone of size $\Delta R = 0.2$ around the direction of each electron candidate. This energy sum excludes cells associated with the electron's cluster and is corrected for leakage from the electron's cluster itself and for energy deposits from pile-up. The tracking isolation variable is based on the sum of the transverse momenta of all tracks around the electron in a cone of size $\Delta R = 0.3$, excluding the electron track. For both isolation variables, requirements are chosen to give separately a 90% electron selection efficiency for electrons from $Z \to ee$ decays in each $p_{\rm T}$ bin.

Muon candidates are identified by matching tracks in the muon spectrometer with tracks in the ID and are required to have $|\eta| < 2.5$ and $p_{\rm T} > 25$ GeV [43, 44]. The longitudinal impact parameter with respect to the primary vertex is required to be less than 2 mm. To reduce the background from muons originating from heavy-flavour decays inside jets, muons are required to be separated by $\Delta R > 0.4$ from the nearest jet and to be isolated. The muon isolation variable, defined as the ratio of the sum of $p_{\rm T}$ of tracks, excluding the muon, in a cone of variable size $\Delta R = 10\,{\rm GeV}/p_{\rm T}(\mu)$, to the $p_{\rm T}$ of the muon is required to be smaller than 0.05 [45]. This isolation requirement results in an efficiency of about 97% for muons from $Z \to \mu\mu$ decays.

Reconstruction of photons [46] starts with forming seed clusters in the EMC with a size 0.075×0.123 in the $\eta \times \phi$ space and with transverse energy above 2.5 GeV using the sliding-window algorithm [47]. Tracks in the ID are matched to EM seed clusters and are used to form conversion-vertex candidates where possible. The conversion-vertex candidates are then matched to the seed clusters. A final algorithm decides whether a seed cluster corresponds to an unconverted photon, a converted photon or a single electron based on the matching to conversion vertices or tracks and on the cluster and track(s) four-momenta. Photon candidates must fulfil identification criteria based on shower-shape variables containing information from the first layer of the EMC (strip layer) [48]. All photons are required to have a transverse momentum of at least 15 GeV and $|\eta_{\rm cl}| < 2.37$, excluding the transition region of the EMC, $1.37 < |\eta_{\rm cl}| < 1.52$.

Jet candidates are reconstructed with the anti-k_t [49] algorithm with a radius parameter $R = 0.4$, using cell clusters [50] in the calorimeter, which are calibrated using the local cluster weighting method [51]. The energies of jets are then calibrated using an energy- and η-dependent simulation-based calibration scheme with in situ corrections based on data. Jets are required to have $p_{\rm T} > 25$ GeV and $|\eta| < 2.5$. To suppress jets from pile-up, a requirement on the jet vertex fraction (JVF) is imposed. It is defined as the ratio of the sum of the $p_{\rm T}$ of tracks associated with both the jet and the primary vertex to the

[2]Events are required to contain a hard collision primary vertex with at least four associated charged particle tracks of $p_{\rm T} > 0.4$ GeV. If there are multiple primary vertices in an event, the one with the largest sum of track $p_{\rm T}^2$ is selected.

JHEP11(2017)086

sum of the p_{T} of all tracks associated with the jet. Jets with $p_{\mathrm{T}} < 50\,\mathrm{GeV}$ and $|\eta| < 2.4$ are required to satisfy $|\mathrm{JVF}| > 0.5$ [52], which achieves high efficiency for jets from hard scatters and high rejection of pile-up jets.

Muons within a cone of $\Delta R = 0.4$ around a jet are removed, as well as the closest jet within a cone of $\Delta R = 0.2$ (0.1) around an electron (photon). Finally, electrons within a cone of $\Delta R = 0.4$ around a jet are removed.

Jets containing b-hadrons are tagged by an algorithm that uses multivariate techniques combining information from the impact parameters of displaced tracks as well as topological properties of secondary and tertiary decay vertices reconstructed within the jet [53–55]. The working point used for this selection corresponds to a 70% efficiency for b-jets with $p_{\mathrm{T}} > 20\,\mathrm{GeV}$ and $|\eta| < 2.5$ in simulated $t\bar{t}$ events, and a light-quark or gluon jet rejection factor of 140.

The missing transverse momentum, with magnitude $E_{\mathrm{T}}^{\mathrm{miss}}$, is reconstructed as the transverse component of the negative vector sum of the momenta of all electrons, muons, photons and jets, as well as calibrated calorimeter energy clusters not associated with any of the above [56].

4.2 Event selection

A single-lepton trigger is used to select the events. For the electron channel, the trigger requires either a p_{T} threshold of 24 GeV and isolation, or a p_{T} threshold of 60 GeV independent of isolation. For the muon channel, the trigger requires a p_{T} threshold of 24 GeV and isolation, or 34 GeV independent of isolation.

In both channels, the presence of exactly one lepton with $p_{\mathrm{T}} > 25\,\mathrm{GeV}$ passing the trigger requirements and at least four jets is required. In order to reduce several background contributions, but mainly the W+jets background, at least one jet is required to be tagged as a b-jet.

For the muon channel, additional requirements on the missing transverse momentum and on m_{T}^{W}, the transverse mass of the W boson candidate [57], $E_{\mathrm{T}}^{\mathrm{miss}} > 20\,\mathrm{GeV}$ and $E_{\mathrm{T}}^{\mathrm{miss}} + m_{\mathrm{T}}^{W} > 60\,\mathrm{GeV}$, are imposed. For the electron channel the requirements are tighter, $E_{\mathrm{T}}^{\mathrm{miss}} > 30\,\mathrm{GeV}$ and $m_{\mathrm{T}}^{W} > 30\,\mathrm{GeV}$, due to the larger multijet background.

The $t\bar{t}\gamma$ candidates are selected by applying the above criteria and by requiring exactly one photon. Events with a jet within a cone of $\Delta R = 0.5$ around the selected photon are rejected to remove photon radiation from quarks. In order to enrich the sample with events in which a photon is radiated from a top quark, the distance between the selected photon and lepton direction is required to be larger than $\Delta R = 0.7$. For the electron channel, the invariant mass of the electron and the photon has to be outside a 5 GeV mass window around the Z boson mass (i.e. $m_{e\gamma} < 86\,\mathrm{GeV}$ or $m_{e\gamma} > 96\,\mathrm{GeV}$) in order to suppress Z+jet events with one electron misidentified as a photon. Additional control regions are defined in section 5.

The selection yields a total of 1256 and 1816 candidate events in the electron and muon channels, respectively. From simulation studies, 440 ± 90 and 720 ± 140 signal events are predicted in the electron and the muon channels, respectively, including all systematic

JHEP11(2017)086

uncertainties discussed in section 8. The photon p_{T} and $|\eta|$ distributions after the selection are shown in figure 1. The data distributions are compared to the predictions from simulation and data-driven estimates for both the signal and backgrounds, as explained in section 6.

For the measurement of the differential cross sections, the phase space in the variables p_{T} and η is divided into five bins each, chosen to be sufficiently large compared to the resolution in the respective variable and to contain a similar number of predicted signal events. The bins in photon p_{T} are 15–25 GeV, 25–40 GeV, 40–60 GeV, 60–100 GeV, and 100–300 GeV, and for the photon $|\eta|$ they are 0–0.25, 0.25–0.55, 0.55–0.90, 0.90–1.37, and 1.37–2.37.

4.3 Definition of the fiducial phase space

The fiducial region for this analysis is defined for Monte Carlo events at particle level (before detector simulation) using the following particle definitions and event selection, which are designed to mimic those at the reconstruction level (after detector simulation). The objects are constructed from stable particles in the event record of the generator with a lifetime larger than 30 ps.

Leptons. Electrons and muons with $p_{\mathrm{T}} > 10$ GeV and $|\eta| < 2.7$ are combined with all photons that do not originate from hadron decays and are within a cone of $\Delta R = 0.1$ and their four-momenta are added together. These modified leptons are then required to have $p_{\mathrm{T}} > 25$ GeV, $|\eta| < 2.5$ and not originate from a hadron decay.

Jets. Jets are clustered with the anti-k_t algorithm with a radius parameter of $R = 0.4$. Neutrinos and muons are not considered in the clustering. Jets are required to have $p_{\mathrm{T}} > 25$ GeV and $|\eta| < 2.5$.

***b*-jets.** Jets are tagged as b-jets if they contain a b-hadron with $p_{\mathrm{T}} > 5$ GeV within $\Delta R = 0.3$ of the jet axis.

Photons. Photons are required to not originate from a hadron decay and to satisfy $E_{\mathrm{T}} > 15$ GeV and $|\eta| < 2.37$.

Overlap removal. The applied overlap removal procedure is the same as for the reconstructed objects, as described in section 4.1.

The following event selection based on the object definitions listed above is applied to define the fiducial phase space: exactly one electron (muon) from a W boson decay is required in the electron (muon) channel; at least four jets have to be selected, among which at least one must be a b-jet; and exactly one photon is required. Additionally, the event is discarded if the photon has $\Delta R(\mathrm{jet}, \gamma) < 0.5$ with any jet or $\Delta R(\ell, \gamma) < 0.7$ where ℓ is the electron or muon.

In order to obtain a common fiducial region for the electron channel and the muon channel, the requirements imposed at the reconstruction level on $E_{\mathrm{T}}^{\mathrm{miss}}$, m_{T}^{W}, and $m_{e\gamma}$ are not included in the fiducial region definition.

JHEP11(2017)086

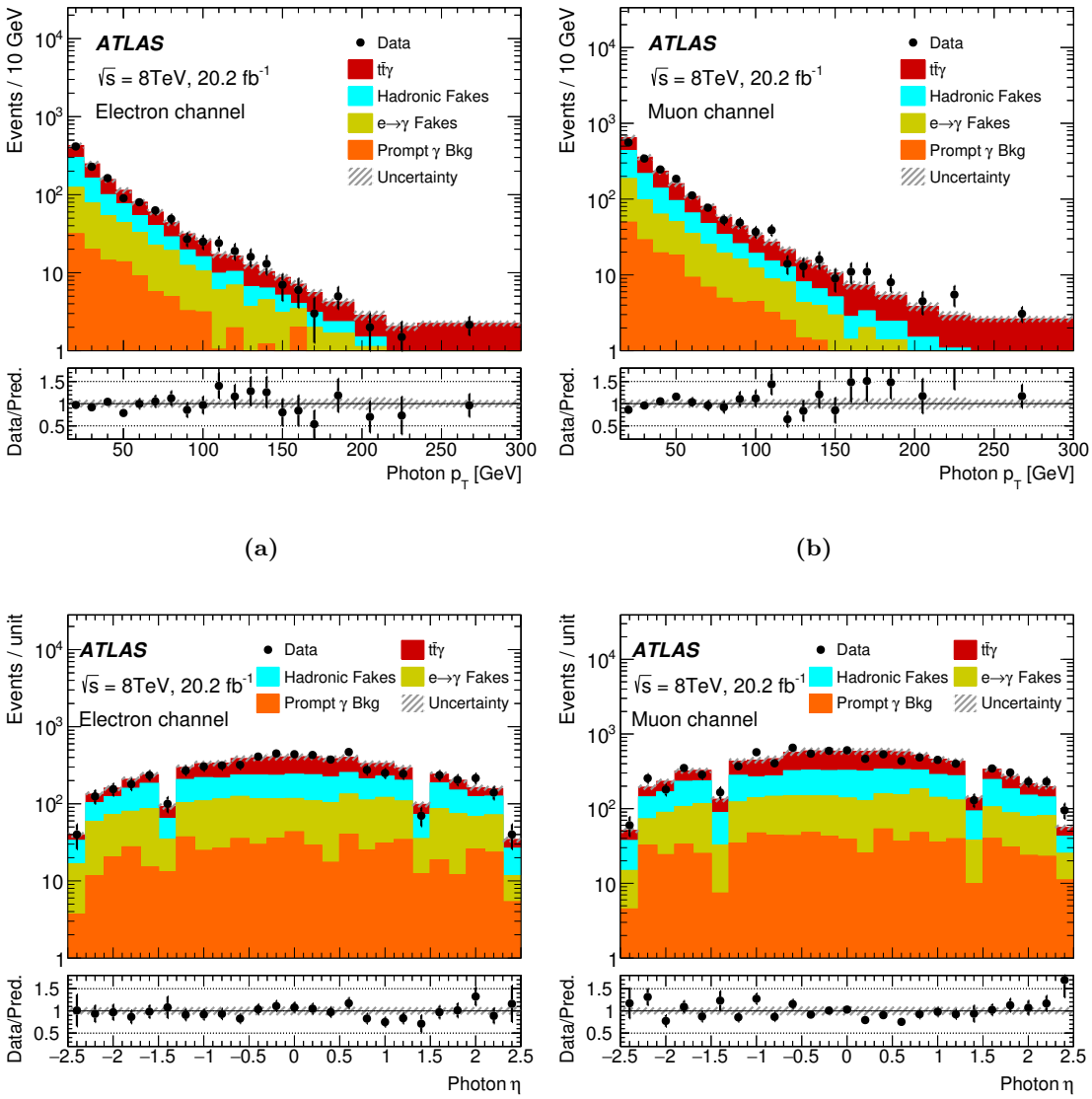

Figure 1. Comparison of data and the expected distributions in the events passing the $t\bar{t}\gamma$ selection for the (a), (c) single-electron channel and (b), (d) single-muon channel. The expected signal and background distributions include the prediction for signal ($t\bar{t}\gamma$), normalised to the next-to-leading-order calculation [9], as well as for other processes with prompt photons, such as $W\gamma$+jets and $Z\gamma$+jets production from simulation (prompt γ bkg), where the $W\gamma$+jets contribution is scaled with a data-driven method. The contributions of events in which an electron is misidentified as a photon ($e \to \gamma$ fakes) and of events in which hadrons are misidentified as photons (hadronic fakes) are estimated from data. The shaded band corresponds to the total uncertainty of the expected signal and backgrounds. Panels (a) and (b) show the photon p_{T} distributions, where the overflow is included in the last bin, while (c) and (d) show the η distributions of the photons.

JHEP11(2017)086

5 Templates

After the event selection there are three classes of events, 1) those with prompt photons, 2) those with photons from hadron decays or hadrons misidentified as photons, called hadronic fakes, and 3) those from electrons misidentified as photons. The prompt-photon category includes both the signal events and other background processes, such as W or Z boson production with prompt photons. The extraction of the total and differential cross sections is based on a likelihood fit using three templates, one for the prompt-photon events, one for the hadronic-fake events and one for electrons misidentified as photons. The normalisations of the first two templates are free parameters in the likelihood fit, while for the third template the normalisation is fixed to the data-driven estimate of the number of events with an electron misidentified as a photon, as described in section 6.2. The variable used for the templates is $p_{\mathrm{T}}^{\mathrm{iso}}$, the sum of the transverse momenta of all tracks within a cone with an opening angle around the photon of 0.2 rad. This variable yields the best discrimination between signal and background and has almost no dependence on the amount of pile-up [8]. A detailed description of the likelihood fit is given in section 7.2, while the background determination is discussed in section 6.

5.1 Prompt-photon template

The prompt-photon template is extracted using the photons from the $t\bar{t}\gamma$ signal simulation after the event selection described in section 4. In addition, only reconstructed photons that are geometrically matched to a particle-level photon within ΔR of 0.1 are selected. Approximately 95% of the photons in the selected signal events fulfil this condition. The prompt-photon template is shown in figure 2. Templates extracted from $W\gamma$+jets and $Z\gamma$+jets simulation are consistent with this template within statistical uncertainties. The simulated sample is large enough to ensure a small statistical uncertainty of the template for the total cross-section measurement, with a maximum uncertainty of 4% in the last bin. For the differential measurements, the template is extracted for each bin of the transverse momentum and pseudorapidity distributions of the photon. In this case, the uncertainty in the last bin of the distribution can be as large as 13%. Both the statistical and systematic uncertainties, discussed in section 8, are taken into account when performing the likelihood fit described in section 7.2.

5.2 Hadronic-fake template

The hadronic-fake template is extracted from a control region in data with at least four jets. Events must have at least one photon candidate that fails to satisfy at least one of the four photon identification criteria constructed using shower-shape variables from the first layer of the EMC. The strip layer is finely segmented in η for suppressing fake photons, which typically have a broader shower profile. While these variables have strong discriminating power between signal and fake photons, they have negligible correlation with the photon isolation [46]. The control region is defined with the same jet multiplicity requirement as for the signal region because the shape of the template depends on the jet multiplicity. In addition, to prevent electrons that are misidentified as photons from entering the control sample, hadronic-fake photon candidates within $\Delta R = 0.1$ of an electron are rejected.

JHEP11(2017)086

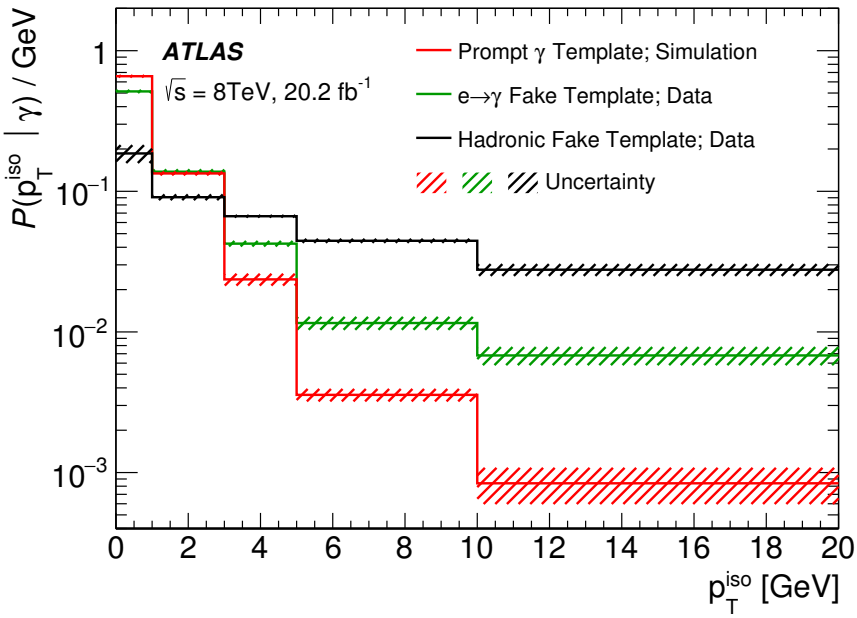

Figure 2. The $p_{\mathrm{T}}^{\mathrm{iso}}$ templates for the inclusive cross-section measurement for prompt photons, hadronic fakes and electron fakes. The template for the signal photon is taken from simulation, while the other two templates are derived from data. The distributions are normalised to unity and the last bins contain the overflows. The shaded bands show the total uncertainty in each template.

The shape of the template depends on both the p_{T} and η of the hadronic fakes. The hadronic fakes are less isolated at higher p_{T} values, as they are more likely to arise from energetic jets which have larger $p_{\mathrm{T}}^{\mathrm{iso}}$ values. The dependence on η is due to the varying amount of material in front of the calorimeter. Because of the different p_{T} and η distributions of the hadronic fakes in the control region and in the signal region, the hadronic-fake template for the total cross-section measurement is calculated as a weighted sum of templates determined in bins of the hadronic fakes: five for p_{T} (here, the same bins as for the photon p_{T} in the differential cross-section measurement are chosen) and two for $|\eta|$ ($|\eta| < 1.80$ and $1.80 < |\eta| < 2.37$). The weights w are the fraction of the hadronic-fake events in a given p_{T} or η range, estimated from another control region in data, closer to the signal region although with fewer events, in order to correct the p_{T} and η distributions of the hadronic fakes. This region is defined exactly in the same way as the signal region, described in section 4, but replacing the nominal photon selection by one where the photon fails to satisfy at least one of the tight identification criteria. The difference in the event topologies between the two control regions was found to have a negligible effect on the final template shape. Since no correlation between p_{T} and η of hadronic fakes is observed in this control region, the dependence of the template on p_{T} and η can be treated separately.

The final weighted hadronic-fake template for the inclusive measurement, shown in figure 2, is calculated according to

$$T_{\mathrm{weighted}}^{\mathrm{h\text{-}fake}} = \frac{1}{2}\left(\sum_{i=1}^{5} w_{p_{\mathrm{T}},i} \;\; T_{p_{\mathrm{T}},i}^{\mathrm{h\text{-}fake}} + \sum_{j=1}^{2} w_{\eta,j} \;\; T_{\eta,j}^{\mathrm{h\text{-}fake}}\right) ,$$

JHEP11(2017)086

where $T^{\text{h-fake}}_{p_{\text{T}},i}$ is the hadronic-fake template of the p_{T} bin i and $w_{p_{\text{T}},i}$ is its corresponding weight, while $T^{\text{h-fake}}_{\eta,j}$ is the hadronic-fake template of the η bin j with $w_{\eta,j}$ as its associated weight. The index i runs over the five bins in p_{T}, while the index j runs over the two bins in η. Similarly, for each bin of the differential cross-section measurement in photon p_{T} (η), a template is obtained by averaging over the hadronic-fake η (p_{T}) dependence.

The main uncertainty in this template stems from a small contamination of the selected events by prompt photons.

5.3 Electron-fake template

Electrons misidentified as photons represent the second-largest background. Electrons and photons have very similar shower shapes in the electromagnetic calorimeter. For this reason, an electron can be misidentified as a photon if the associated track is poorly reconstructed, or in case of nearby jet activity it can be misidentified as a converted photon. A $p_{\text{T}}^{\text{iso}}$ template is derived from photons in a control sample containing electron-photon pairs with an invariant mass compatible with the Z boson mass, hereafter called $Z \to e + \text{fake } \gamma$ events. In these events the photon is predominantly an electron misidentified as a photon. The control sample selection requires an electron and a photon with an opening angle larger than 150° and an invariant mass in the range 70–110 GeV. The p_{T} of the electron has to be larger than that of the photon. In order to select events with a topology close to the signal events, a requirement of $E_{\text{T}}^{\text{miss}} > 30\,\text{GeV}$ is applied. Other backgrounds in this region are estimated from a sideband fit to the $m_{e\gamma}$ distribution modelled by a Gaussian function. The corresponding template, after background subtraction, is shown in figure 2.

6 Background estimation

Several background processes can mimic the $t\bar{t}\gamma$ signature of the signal events. In order of importance the main background contributions are fake photons from misidentified hadrons, predominantly in $t\bar{t}$ events (section 6.1), and events with electrons misidentified as photons (section 6.2). Further small contributions stem from processes with prompt photons (section 6.3). The sizes of the background contributions are given in section 9.

6.1 Background from hadrons misidentified as photons

The main background contribution to the $t\bar{t}\gamma$ process comes from hadrons, or photons from hadron decays, that are misidentified as prompt photons. This background is estimated from data using the template fit. The main photon background contribution is $t\bar{t}$ production with one hadronic fake. The derivation of the template used for the hadrons misidentified as photons is described in section 5.2.

6.2 Background from electrons misidentified as photons

Events with electrons misidentified as photons are the second largest background contribution. The main contribution arises from $t\bar{t}$ events with both top quarks decaying semileptonically thereby producing two electrons or one electron and one muon. The second largest contribution is Z+jets production where the Z boson decays into an e^+e^-

JHEP11(2017)086

pair and one of the electrons is misidentified as a photon. The contribution of events with electrons misidentified as photons is estimated with a fully data-driven method.

The probability for an electron to fake a photon (fake rate) is calculated using two control regions, one enriched in $Z \to ee$ and one enriched in events reconstructed as $Z \to e + \text{fake}\,\gamma$ events. The event selections for the $Z \to ee$ and $Z \to e + \text{fake}\,\gamma$ samples require two back-to-back objects, either two electrons or an electron and a photon. The definitions are the same as for the signal selection except for the second electron in the $Z \to ee$ selection, where the p_{T} threshold is lowered from 25 GeV to 15 GeV so that it is the same as for the photon. In the $Z \to e + \text{fake}\,\gamma$ selection the electron is required to have a larger p_{T} than the photon. In both selections the object with the larger p_{T} is the tag while the other one is the probe, i.e. the tag is always an electron.

The numbers of $Z \to ee$ and $Z \to e + \text{fake}\,\gamma$ events are determined from a fit of the invariant mass distribution of the two objects using a sum of a Crystal-Ball [58] and a Gaussian function. The fit is performed in the region where the invariant mass lies between 70 GeV and 110 GeV. The fake rate is calculated from the ratio of these two numbers, as a function of the transverse energy and the pseudorapidity of the photon. A correction accounting for the different reconstruction and identification efficiencies for electrons and photons is applied.

The contribution of electrons reconstructed as photons in the signal region is then estimated by applying the fake rate to a modified signal region, where an electron fulfilling the same kinematic selection as the photon is required. This background contributes $317 \pm 7 \pm 41$ and $385 \pm 6 \pm 42$ events in the electron and muon channels, respectively, where the first error is statistical and the second is systematic. The systematic uncertainty is estimated by varying the range and functions used in the fit of the two invariant mass distributions.

6.3 Background events with a prompt photon

There are several background processes to $t\bar{t}$ production that can become a background to the $t\bar{t}\gamma$ sample, if an additional prompt photon is present.

Multijet production with an associated prompt photon is a source of background when one of the jets in the event is misidentified as a lepton, referred to as a fake lepton. In order to estimate this background, a control sample is created that uses the same event selection as for the signal except that the lepton identification criteria are loosened. To account for the sample composition in fake and real leptons, each event is assigned a weight computed from the matrix method [57] in order to obtain a distribution corresponding to fake leptons. To calculate the contribution of events with a prompt photon in this sample, a likelihood fit is performed on the $p_{\mathrm{T}}^{\mathrm{iso}}$ distribution of these weighted events, using the prompt-photon and hadron-fake templates described in section 5.1 and section 5.2, respectively. This results in estimated background contributions of 7.5 ± 3.6 events in the electron channel and 8.3 ± 5.2 events in the muon channel. The uncertainties are purely statistical.

Additional backgrounds from $W\gamma$+jets, $Z\gamma$+jets, single top quark and diboson production are estimated using Monte Carlo simulations. For the $W\gamma$+jets events, the cross sections from simulation do not agree with the data, as the fraction of heavy-flavour jets

JHEP11(2017)086

Process	e + jets	μ + jets
Multijet + γ	7.5 ± 3.6	8.3 ± 5.2
$W\gamma$+jets	65 ± 25	97 ± 25
$Z\gamma$+jets	35 ± 19	38 ± 20
Single top + γ	13 ± 7	19 ± 10
Diboson + γ	2.6 ± 1.5	2.5 ± 1.4

Table 1. Expected yields of background processes with a prompt photon. The uncertainties include all sources of systematic uncertainty described in section 8.

observed in data is smaller than the prediction obtained using the Sherpa generator, and thus a scale factor is applied to the prediction of the simulation. This scale factor is derived from a control region in data and is 0.69 ± 0.16 for the electron channel and 0.76 ± 0.14 for the muon channel. The control region is defined exactly as for the signal region, except for the required number of jets (between one and three), the number of b-tagged jets (exactly one), and for an additional requirement on the invariant mass of the lepton and the photon, which has to be less than 40 GeV. The uncertainties include the statistical and systematic uncertainty induced by the subtraction of the non-$W\gamma$+jets events from the control region. A comparison between Alpgen and the nominal generation with Sherpa gives an additional 20% uncertainty. For the $Z\gamma$+jets, single-top and diboson production with an additional photon, a 50% theoretical uncertainty is assumed. In addition, all uncertainties discussed in section 8 are taken into account.

The expected yields for these backgrounds are summarised in table 1.

7 Measurement of the fiducial cross section

In this section, the theoretical predictions for the fiducial region $t\bar{t}\gamma$ cross section and differential cross sections are described. The fit strategy used to extract these from the data is also presented.

7.1 Theoretical prediction

Production cross sections of a top-quark pair in association with a prompt photon have been calculated at NLO in QCD [9], extending calculations obtained assuming stable top quarks [59]. While the results presented in ref. [9] were calculated at a centre-of-mass energy of $\sqrt{s} = 14$ TeV, a dedicated calculation at $\sqrt{s} = 8$ TeV has been performed in the single-lepton channel both at LO and NLO using the same techniques as in ref. [9]. The `CTEQ6L1` (`CT10`) PDF set is used for the LO (NLO) calculation, while for both a fine-structure constant $\alpha = 1/137$ and renormalisation and factorisation scales $\mu_{\mathrm{R}} = \mu_{\mathrm{F}} = m_{\mathrm{top}}$ are used. Further computations were performed by simultaneously varying the scales μ_{R} and μ_{F} by a factor of 2 or 0.5. The LO calculation agrees with the cross section from MadGraph within 2%, for scale choices of both m_{top} and $2m_{\mathrm{top}}$. The ratio of the NLO and LO cross sections, known as the K-factor, is obtained from the NLO theory calculation at a scale of m_{top} and the LO MadGraph sample at a scale of $2m_{\mathrm{top}}$, after applying the restricted

JHEP11(2017)086

phase space requirements described in section 3. The overall K-factor was calculated to be $K = 1.90 \pm 0.25 \pm 0.12$, with the first uncertainty accounting for scale variation and the second for PDF set variation. For the differential cross-section predictions, the K-factors for the corresponding bin in p_{T} or η are used. These K-factors are used to correct the prediction from simulation with MadGraph.

The K-factor derived above is then used to calculate the cross section at NLO by using only events from the simulation with MadGraph in the same fiducial region as defined in section 4.3. The inclusive cross section is calculated to be 151 ± 24 fb. In addition, the cross section is calculated in bins of p_{T} and η with the same fiducial requirements as for the cross-section measurement.

7.2 Fit strategy

The cross section for $t\bar{t}\gamma$ production is extracted from the observed binned $p_{\mathrm{T}}^{\mathrm{iso}}$ distribution employing a likelihood fit. There are two free parameters in the fit, i.e. the total number of signal events and the total number of hadronic-fake events. The $p_{\mathrm{T}}^{\mathrm{iso}}$ templates used in the fit are shown in figure 2. The prompt-photon template is used for the signal and all backgrounds with a prompt photon. For the background from electrons misidentified as photons, the electron-fake template is utilised and for hadronic fakes the hadronic-fake template is utilised. All backgrounds, except for the hadronic fakes, are described by a Poisson probability distribution with the mean values determined in section 6.

The likelihood function $\mathcal{L}$ is defined as the product

$$\mathcal{L} = \prod_{i,j} P\left(N_{i,j} | N_{i,j}^{s} + \sum_{b} N_{i,j}^{b}\right) \cdot \prod_{t} G(0|\theta_t, 1). \tag{7.1}$$

The Poisson function $P(N_{i,j}|N_{i,j}^{s} + \sum_b N_{i,j}^{b})$ models the event yield in bin j of the $p_{\mathrm{T}}^{\mathrm{iso}}$ distribution of bin i of the p_{T} or η distribution, where $N_{i,j}$ is the observed number of events and $N_{i,j}^{s}$ and $N_{i,j}^{b}$ are the expected numbers of signal and background events. There is only one bin for the inclusive measurement, while there are five bins for each of the differential cross-section measurements, corresponding to the bins in photon p_{T} or η. The Gaussian function $G(0|\theta_t, 1)$ of unit width models the systematic uncertainty t, where θ_t is the parameterisation of this uncertainty. The sources of systematic uncertainty are discussed in section 8.

The inclusive and differential fiducial cross sections are related to the number of signal events by

$$L \cdot \sigma_i \cdot C_i \cdot f_{i,j} = N_{i,j}^{s},$$

where L is the integrated luminosity of the data sample, σ_i is the fiducial cross section to be determined, $f_{i,j}$ is the fraction of events falling into bin j of $p_{\mathrm{T}}^{\mathrm{iso}}$ of bin i, calculated from the signal template, and C_i is the ratio of the number of reconstructed events to the number of generated events in the fiducial region in bin i. The term C_i can also be expressed as the ratio of the number of reconstructed events to the number of reconstructed events falling into the fiducial region in bin i, multiplied by the signal efficiency. The ratio C_i therefore corrects for the event selection efficiency and the migration of events between the fiducial

JHEP11(2017)086

and the non-fiducial region, including leptonic τ decays, or between different bins i, in the case of the differential cross-section measurement. The values of C_i range from 0.21 to 0.38 (0.38 to 0.62) for the electron (muon) channel, depending on the bin in p_{T} or η. For the differential cross-section measurements, this means that the cross section σ_i is computed in each bin i using a bin-by-bin unfolding.

To consider the effect of a systematic uncertainty t on the value of a parameter p in the fit, p is multiplied by a response function, which is a function of the nuisance parameter θ_t used to parameterise this uncertainty. The parameters are the variables used to calculate $N^s_{i,j}$ or $N^b_{i,j}$,

$$p(\theta_t) = p \cdot (1 + \sigma_p)^{\theta_t},$$

where σ_p is the uncertainty of parameter p due to the systematic uncertainty t. There could be multiple response functions multiplying p, if it is affected by more than one systematic uncertainty.

The fiducial cross sections are extracted by maximising the likelihood function (eq. (7.1)). To obtain the confidence interval for the fitted cross sections, a profile likelihood ratio λ_s is built according to

$$\lambda_s(\sigma) = \frac{\mathcal{L}(\sigma, \hat{\hat{\boldsymbol{\theta}}})}{\mathcal{L}(\hat{\sigma}, \hat{\boldsymbol{\theta}})},$$

where the nuisance parameters are denoted by $\boldsymbol{\theta}$. The quantities with single hats are their unconditional maximum-likelihood estimate, while the quantities with double hats are their conditional maximum-likelihood estimate when σ is fixed. The profile likelihood ratio is evaluated within the RooFit/RooStats framework [60, 61] and used to determine the upper and lower limits on the cross section at the 68% confidence level. In the fit, events from the electron and muon channels are merged, having a common parameter of interest, i.e. the fiducial cross section.

For the differential cross-section measurement, the fiducial region definition includes all the requirements for the total cross-section measurement. In addition, the true p_{T} or η of the photon has to be in the bin considered. The systematic uncertainties are treated as correlated between the bins. The size of the bins is chosen to keep the migration between bins lower than the expected statistical uncertainty of the cross-section measurement in that bin, in order to have only a small contribution from the bin-by-bin unfolding to the total uncertainty. The migration between bins is smaller than 7% for all bins.

8 Systematic uncertainties

There are three categories of systematic uncertainty affecting the results: the modelling uncertainties, the experimental uncertainties, and the uncertainties related to the template shapes. When varying the parameters to estimate uncertainties, only small differences between the positive and negative uncertainties in the cross section are observed. The uncertainty is therefore symmetrised by taking the larger of the two values. The uncertainties for the inclusive and differential measurements are derived in the same way. The uncertainties for the inclusive measurement are discussed in detail below and summarised in table 2. The uncertainties for the differential measurements are included in table 3.

JHEP11(2017)086

8.1 Modelling uncertainties

The renormalisation and factorisation scales for the simulation of the signal process are varied simultaneously from their nominal value of $\mu_{\mathrm{R}} = \mu_{\mathrm{F}} = 2m_{\mathrm{top}}$ by a factor of 1/2 or 2, resulting in an uncertainty of 0.6% in the measured cross section. Pythia 6, which is used for the nominal signal sample, is replaced by Herwig 6.520 [30] and Jimmy 4.31 [31] to estimate the uncertainty due to the modelling of the parton shower, underlying event, and hadronisation. This results in an uncertainty of 0.6% in the cross section. Initial- and final-state radiation are studied by using Pythia 6 tunes with high (`Perugia2011C radHi`) and low (`Perugia2011C radLo`) QCD radiation activity for the signal sample. This results in an uncertainty in the inclusive cross section of 2.2%.

Other signal modelling uncertainties were studied, including the choice of matrix-element event generator [8], the PDF, and the effect of colour reconnection, underlying event, and QED uncertainties, and are found to be negligible. The uncertainties in the $Z\gamma$+jets, single-top+γ and diboson+γ backgrounds are estimated using the 48% uncertainty in the normalisation of the samples in the four-jet bin from the Berends-Giele scaling [62]. For the $Z\gamma$+jets events, this is the largest uncertainty, resulting in an uncertainty of 2.8% in the inclusive cross-section measurement. For the single-top+γ events the uncertainty is 1.2%, while for the diboson+γ events the uncertainty is negligible.

For $W\gamma$+jets events, the uncertainty in the scale factor used to normalise the sample (section 6.3), as well as the difference between the predictions from Sherpa and Alpgen, is taken into account, resulting in a total uncertainty of 4.0%.

The fake rate used to estimate the background from electrons misidentified as photons shows a dependence on the choice of range and function used in the fit of the ee and $e\gamma$ invariant mass distributions, resulting in a total systematic uncertainty of 6.1% in the measured inclusive cross section.

8.2 Experimental uncertainties

Experimental uncertainties common to signal and background processes come mainly from the uncertainties associated with the event reconstruction, identification, and trigger efficiencies, momentum and energy scales, and momentum and energy resolutions of the jets, the photon, the lepton, and $E_{\mathrm{T}}^{\mathrm{miss}}$. In addition, the uncertainties associated with the jet flavour tagging, the integrated luminosity, and the pile-up simulation are considered.

The largest uncertainty associated with jets arises from the jet energy scale (JES) [63], which is split into several independent categories. To determine the JES uncertainty, each source is varied independently, and the results added in quadrature to obtain an uncertainty in the inclusive cross section of 4.9%. The leading sources for the JES uncertainty are due to uncertainties in the modelling, the amount of pile-up, and the jet flavour composition. The jet energy resolution is evaluated in a similar way [64] and results in a total uncertainty of 0.5%.

The photon identification efficiency [46] is measured with samples of photons from the radiative decays of the Z boson, and electrons and positrons from Z boson decays, exploiting the similarity between electron and photon electromagnetic showers. Scale factors

JHEP11(2017)086

are used to correct for detector mismodelling. Uncertainties in these scale factors range between 1.5% and 2.5% (2% and 3%) for unconverted (converted) photons in the region of $E_{\mathrm{T}} < 40\,\mathrm{GeV}$, and 0.5% to 1% for higher transverse energies. These scale factors are varied to study their impact on the analysis, resulting in an uncertainty in the inclusive cross section of 1.2%. The photon energy scale uncertainty [48] contributes another 0.7% uncertainty to the measured inclusive cross section.

For leptons, the trigger and identification efficiencies, and the energy scale and resolution have been investigated [42, 44, 64]. Correction factors that are applied to the simulation to better match the data are varied within their uncertainty, resulting in an uncertainty of 1.1% in the total cross-section measurement.

The uncertainty in b-tagging [53] is accounted for by varying the calibration scale factors for b-jets, c-jets, and light-flavour jets by their corresponding systematic uncertainties independently yielding a total systematic uncertainty of 0.3%. The contribution due to the $E_{\mathrm{T}}^{\mathrm{miss}}$ uncertainty is negligible.

The uncertainty in the integrated luminosity is 1.9%, as determined from a calibration of the luminosity scale derived from beam-separation scans [40]. As the luminosity affects both the signal and background normalisation the resulting uncertainty is 2.1%.

8.3 Template-related uncertainties

The dominant uncertainty in the hadron-fake template comes from the contamination by prompt photons. In order to take this contamination into account, a modified template is constructed, where the photon candidates are required not only to fail one of the photon identification requirements based on shower shapes, but all four of them (section 5.2). The likelihood fit is then repeated using the modified template resulting in a systematic uncertainty in the inclusive cross section of 6.3%.

The prompt-photon template is affected by the modelling and experimental systematic uncertainties as described in sections 8.1 and 8.2.

The largest uncertainty due to the template describing electrons misidentified as photons comes from a variation on the $E_{\mathrm{T}}^{\mathrm{miss}}$ requirement in the event selection. Other uncertainties are due to the variation of the mass range in the event selection and the p_{T} ordering chosen in the determination of the electron fake rates. The combination of these effects, together with the fake rate uncertainty introduced above, yields a systematics uncertainty of 6.3% on the cross section measurement.

9 Results

A total of 3072 candidate events are observed in data. The result of the fit in the fiducial region for the inclusive cross section is summarised in table 3, together with the event yields of the backgrounds. No significant pull of the fit input values and their uncertainties is observed compared to the post-fit values. Also, the fitted event yields for the differential cross-section measurement are shown in each photon p_{T} and η bin.

The post-fit track isolation distribution for the inclusive measurement is shown in figure 3a.

JHEP11(2017)086

Source	Relative uncertainty [%]
Hadron-fake template	6.3
$e \to \gamma$ fake	6.3
Jet energy scale	4.9
$W\gamma$+jets	4.0
$Z\gamma$+jets	2.8
Initial- and final-state radiation	2.2
Luminosity	2.1
Photon	1.4
Single top+γ	1.2
Muon	1.2
Electron	1.0
Scale uncertainty	0.6
Parton shower	0.6
Statistical uncertainty	5.1
Total uncertainty	13

Table 2. List of the most important systematic uncertainties for signal and background and their effects on the measurement of the inclusive cross section. In addition, the statistical and total uncertainty are given. The total uncertainty is derived from the likelihood fit.

Range	$t\bar{t}\gamma$	Hadronic fake	$e \to \gamma$ fake	$W\gamma$+jets	$Z\gamma$+jets	Single top+γ	Multijet+γ	Diboson+γ	Data
Total	1060 ± 130	1020 ± 90	710 ± 90	160 ± 40	73 ± 32	32 ± 15	16 ± 6	5.1 ± 2.4	3072
$15 \leq p_{\mathrm{T}} < 25$ GeV	280 ± 40	360 ± 40	240 ± 35	47 ± 13	23 ± 10	7 ± 4	4.4 ± 2.3	1.3 ± 0.7	966
$25 \leq p_{\mathrm{T}} < 40$ GeV	309 ± 34	233 ± 26	171 ± 7	37 ± 10	22 ± 10	6.4 ± 3.3	3.8 ± 2.4	1.8 ± 0.9	783
$40 \leq p_{\mathrm{T}} < 60$ GeV	220 ± 40	205 ± 21	111 ± 30	28 ± 8	13 ± 6	10 ± 5	1.6 ± 1.9	0.5 ± 0.3	589
$60 \leq p_{\mathrm{T}} < 100$ GeV	160 ± 40	116 ± 16	100 ± 40	24 ± 7	10 ± 5	8 ± 4	3.4 ± 2.1	1.0 ± 0.6	420
$100 \leq p_{\mathrm{T}} < 300$ GeV	150 ± 25	71 ± 10	50 ± 20	23 ± 7	4 ± 2	0.9 ± 0.7	0.8 ± 1.0	0.3 ± 0.2	298
$\lvert\eta\rvert < 0.25$	246 ± 34	121 ± 21	93 ± 24	18 ± 6	9 ± 4	4.0 ± 2.2	5.2 ± 1.8	1.0 ± 0.6	497
$0.25 \leq \lvert\eta\rvert < 0.55$	260 ± 40	130 ± 20	116 ± 29	29 ± 8	11 ± 6	3.7 ± 2.1	0.0 ± 0.4	1.5 ± 0.8	552
$0.55 \leq \lvert\eta\rvert < 0.90$	180 ± 40	198 ± 27	150 ± 40	31 ± 9	16 ± 7	2.2 ± 1.3	4.0 ± 1.8	0.4 ± 0.2	578
$0.90 \leq \lvert\eta\rvert < 1.37$	200 ± 40	233 ± 33	169 ± 50	35 ± 10	17 ± 8	9 ± 5	5.7 ± 2.1	1.0 ± 0.5	663
$1.37 \leq \lvert\eta\rvert < 2.37$	150 ± 40	344 ± 33	200 ± 12	48 ± 13	19 ± 9	13 ± 6	5.4 ± 2.5	1.4 ± 0.7	782

Table 3. Post-fit event yields for the signal and backgrounds for the inclusive cross-section measurement and for the different bins of reconstructed photon p_{T} and η for the differential cross-section measurement. The uncertainties include the statistical and systematic uncertainties.

JHEP11(2017)086

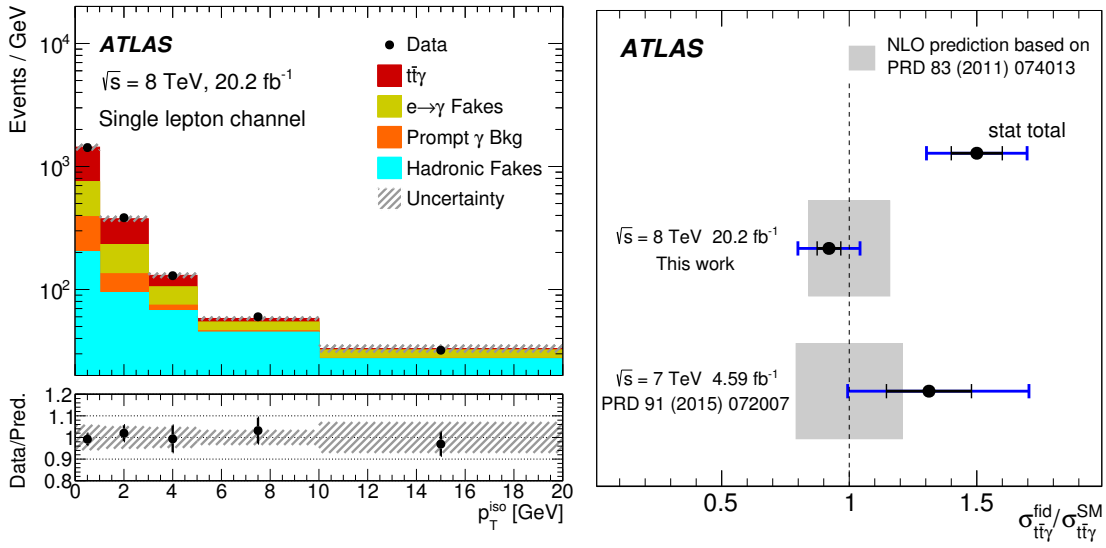

(a) (b)

Figure 3. (a) Post-fit track isolation distribution for the inclusive cross-section measurement. The last bin includes the overflow. The uncertainty band includes all uncertainties. (b) Summary of fiducial measurements of $t\bar{t}\gamma$ production in pp collisions at 7 TeV [8] and 8 TeV, normalised to the expected cross section, calculated at NLO accuracy [9].

Using data selected in the single-lepton channel, the result of the inclusive measurement is:

$$\sigma_{\rm sl}^{\rm fid} = 139 \pm 7\ (\text{stat.}) \pm 17\ (\text{syst.})\ \text{fb} = 139 \pm 18\ \text{fb},$$

which agrees with the NLO prediction of 151 ± 24 fb [9]. This result is compared to the Standard Model calculation as well as to the measurement performed at $\sqrt{s} = 7$ TeV [8] in figure 3b. Good agreement with the NLO predictions is observed in both cases.

The measured $p_{\rm T}$ and η differential cross sections are shown and compared with their corresponding theoretical predictions in figure 4. Good agreement is observed between the measurement and predicted values.

10 Conclusions

A measurement of the fiducial cross section of top-quark pair events in association with a photon, using 20.2 fb^{-1} of 8 TeV pp collision data collected in 2012 by the ATLAS detector at the LHC is presented. The measurement is performed in the single-lepton channel with either one isolated electron or muon, at least four jets where at least one is b-tagged in the fiducial region $p_{\rm T}(\gamma) > 15$ GeV, $|\eta(\gamma)| < 2.37$ and $p_{\rm T}(\ell) > 25$ GeV, $|\eta(\ell)| < 2.5$, with angular separations $\Delta R(\ell, \gamma) > 0.7$ and $\Delta R(\text{jet}, \gamma) > 0.5$. The result is based on the minimisation of a profile likelihood ratio, using the photon track isolation as the discriminating variable since it provides good rejection against the main background of hadronic

JHEP11(2017)086

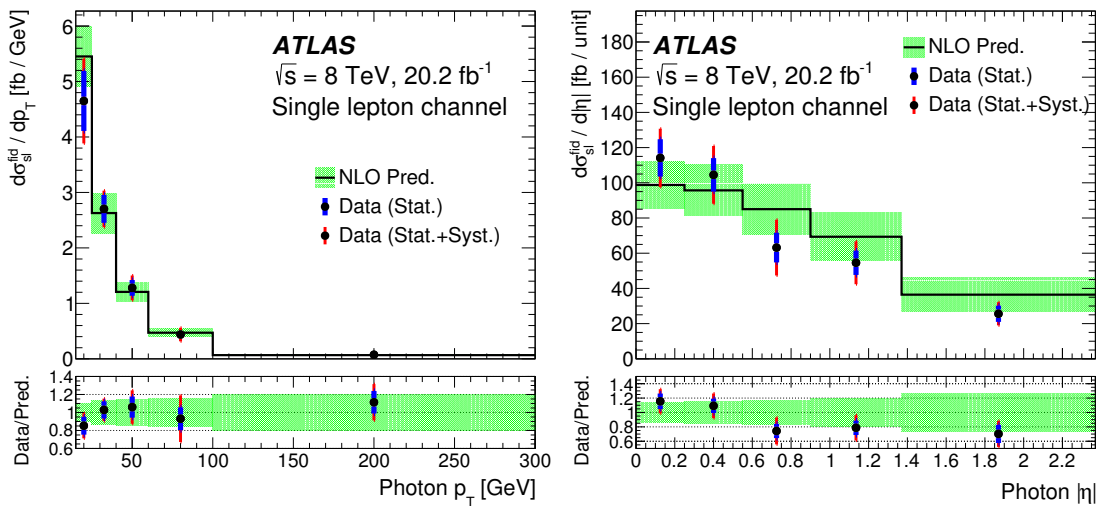

(a) (b)

Figure 4. Measured differential cross section in (a) p_{T} and (b) $|\eta|$ and the corresponding theoretical prediction.

jets misidentified as photons. The analysis uses data-driven measurements for the determination of the largest background contributions. In particular, the track isolation template of the hadronic fakes and the background contributions of electron fakes and QCD multijet events are obtained from data.

The fiducial $t\bar{t}\gamma$ cross section is extracted by a combined fit using the single-lepton channel and the theoretical prediction at NLO is in agreement with this measurement. In addition differential cross sections with respect to photon p_{T} and η are measured. These results also agree with the theoretical predictions at NLO within uncertainties.

Acknowledgments

We thank CERN for the very successful operation of the LHC, as well as the support staff from our institutions without whom ATLAS could not be operated efficiently.

We acknowledge the support of ANPCyT, Argentina; YerPhI, Armenia; ARC, Australia; BMWFW and FWF, Austria; ANAS, Azerbaijan; SSTC, Belarus; CNPq and FAPESP, Brazil; NSERC, NRC and CFI, Canada; CERN; CONICYT, Chile; CAS, MOST and NSFC, China; COLCIENCIAS, Colombia; MSMT CR, MPO CR and VSC CR, Czech Republic; DNRF and DNSRC, Denmark; IN2P3-CNRS, CEA-DSM/IRFU, France; SRNSF, Georgia; BMBF, HGF, and MPG, Germany; GSRT, Greece; RGC, Hong Kong SAR, China; ISF, I-CORE and Benoziyo Center, Israel; INFN, Italy; MEXT and JSPS, Japan; CNRST, Morocco; NWO, Netherlands; RCN, Norway; MNiSW and NCN, Poland; FCT, Portugal; MNE/IFA, Romania; MES of Russia and NRC KI, Russian Federation; JINR; MESTD, Serbia; MSSR, Slovakia; ARRS and MIZŠ, Slovenia; DST/NRF, South Africa; MINECO, Spain; SRC and Wallenberg Foundation, Sweden; SERI, SNSF and

JHEP11(2017)086

Cantons of Bern and Geneva, Switzerland; MOST, Taiwan; TAEK, Turkey; STFC, United Kingdom; DOE and NSF, United States of America. In addition, individual groups and members have received support from BCKDF, the Canada Council, CANARIE, CRC, Compute Canada, FQRNT, and the Ontario Innovation Trust, Canada; EPLANET, ERC, ERDF, FP7, Horizon 2020 and Marie Skłodowska-Curie Actions, European Union; Investissements d'Avenir Labex and Idex, ANR, Région Auvergne and Fondation Partager le Savoir, France; DFG and AvH Foundation, Germany; Herakleitos, Thales and Aristeia programmes co-financed by EU-ESF and the Greek NSRF; BSF, GIF and Minerva, Israel; BRF, Norway; CERCA Programme Generalitat de Catalunya, Generalitat Valenciana, Spain; the Royal Society and Leverhulme Trust, United Kingdom.

The crucial computing support from all WLCG partners is acknowledged gratefully, in particular from CERN, the ATLAS Tier-1 facilities at TRIUMF (Canada), NDGF (Denmark, Norway, Sweden), CC-IN2P3 (France), KIT/GridKA (Germany), INFN-CNAF (Italy), NL-T1 (Netherlands), PIC (Spain), ASGC (Taiwan), RAL (U.K.) and BNL (U.S.A.), the Tier-2 facilities worldwide and large non-WLCG resource providers. Major contributors of computing resources are listed in ref. [65].

Open Access. This article is distributed under the terms of the Creative Commons Attribution License (CC-BY 4.0), which permits any use, distribution and reproduction in any medium, provided the original author(s) and source are credited.

References

[1] U. Baur, A. Juste, L.H. Orr and D. Rainwater, *Probing electroweak top quark couplings at hadron colliders*, *Phys. Rev.* **D 71** (2005) 054013 [hep-ph/0412021] [INSPIRE].

[2] A.O. Bouzas and F. Larios, *Electromagnetic dipole moments of the top quark*, *Phys. Rev.* **D 87** (2013) 074015 [arXiv:1212.6575] [INSPIRE].

[3] R. Röntsch and M. Schulze, *Probing top-Z dipole moments at the LHC and ILC*, *JHEP* **08** (2015) 044 [arXiv:1501.05939] [INSPIRE].

[4] M. Schulze and Y. Soreq, *Pinning down electroweak dipole operators of the top quark*, *Eur. Phys. J.* **C 76** (2016) 466 [arXiv:1603.08911] [INSPIRE].

[5] O. Bessidskaia Bylund, F. Maltoni, I. Tsinikos, E. Vryonidou and C. Zhang, *Probing top quark neutral couplings in the Standard Model Effective Field Theory at NLO in QCD*, *JHEP* **05** (2016) 052 [arXiv:1601.08193] [INSPIRE].

[6] P.-F. Duan, Y. Zhang, Y. Wang, M. Song and G. Li, *Electroweak corrections to top quark pair production in association with a hard photon at hadron colliders*, *Phys. Lett.* **B 766** (2017) 102 [arXiv:1612.00248] [INSPIRE].

[7] CDF collaboration, T. Aaltonen et al., *Evidence for $t\bar{t}\gamma$ production and measurement of $\sigma_{t\bar{t}\gamma}/\sigma_{t\bar{t}}$*, *Phys. Rev.* **D 84** (2011) 031104(R) [arXiv:1106.3970] [INSPIRE].

[8] ATLAS collaboration, *Observation of top-quark pair production in association with a photon and measurement of the $t\bar{t}\gamma$ production cross section in pp collisions at $\sqrt{s} = 7$ TeV using the ATLAS detector*, *Phys. Rev.* **D 91** (2015) 072007 [arXiv:1502.00586] [INSPIRE].

JHEP11(2017)086

[9] K. Melnikov, M. Schulze and A. Scharf, *QCD corrections to top quark pair production in association with a photon at hadron colliders*, *Phys. Rev.* **D 83** (2011) 074013 [arXiv:1102.1967] [INSPIRE].

[10] ATLAS collaboration, *The ATLAS Experiment at the CERN Large Hadron Collider*, 2008 *JINST* **3** S08003 [INSPIRE].

[11] T. Sjöstrand, S. Mrenna and P. Skands, *A brief introduction to PYTHIA 8.1*, *Comput. Phys. Commun.* **178** (2008) 852 [arXiv:0710.3820] [INSPIRE].

[12] A.D. Martin, W.J. Stirling, R.S. Thorne and G. Watt, *Parton distributions for the LHC*, *Eur. Phys. J.* **C 63** (2009) 189 [arXiv:0901.0002] [INSPIRE].

[13] ATLAS collaboration, *Summary of ATLAS PYTHIA 8 tunes*, ATL-PHYS-PUB-2012-003 [INSPIRE].

[14] J. Alwall et al., *The automated computation of tree-level and next-to-leading order differential cross sections, and their matching to parton shower simulations*, *JHEP* **07** (2014) 079 [arXiv:1405.0301] [INSPIRE].

[15] T. Sjöstrand, S. Mrenna and P. Skands, *PYTHIA 6.4 physics and manual*, *JHEP* **05** (2006) 026 [hep-ph/0603175] [INSPIRE].

[16] ATLAS collaboration, *Measurement of $t\bar{t}$ production with a veto on additional central jet activity in pp collisions at $\sqrt{s} = 7$ TeV using the ATLAS detector*, *Eur. Phys. J.* **C 72** (2012) 2043 [arXiv:1203.5015] [INSPIRE].

[17] J. Pumplin et al., *New generation of parton distributions with uncertainties from global QCD analysis*, *JHEP* **07** (2002) 012 [hep-ph/0201195] [INSPIRE].

[18] P.Z. Skands, *Tuning Monte Carlo generators: The Perugia tunes*, *Phys. Rev.* **D 82** (2010) 074018 [arXiv:1005.3457] [INSPIRE].

[19] E. Barberio and Z. Wąs, *PHOTOS: A universal Monte Carlo for QED radiative corrections: version 2.0*, *Comput. Phys. Commun.* **79** (1994) 291 [INSPIRE].

[20] P. Golonka and Z. Wąs, *PHOTOS Monte Carlo: a precision tool for QED corrections in Z and W decays*, *Eur. Phys. J.* **C 45** (2006) 97 [hep-ph/0506026] [INSPIRE].

[21] P. Golonka, B. Kerševan, T. Pierzchała, E. Richter-Wąs, Z. Wąs and M. Worek, *The tauola-photos-F environment for the TAUOLA and PHOTOS packages, release II*, *Comput. Phys. Commun.* **174** (2006) 818 [hep-ph/0312240] [INSPIRE].

[22] T. Gleisberg et al., *Event generation with SHERPA 1.1*, *JHEP* **02** (2009) 007 [arXiv:0811.4622] [INSPIRE].

[23] H.-L. Lai et al., *New parton distributions for collider physics*, *Phys. Rev.* **D 82** (2010) 074024 [arXiv:1007.2241] [INSPIRE].

[24] M.L. Mangano, M. Moretti, F. Piccinini, R. Pittau and A.D. Polosa, *ALPGEN, a generator for hard multiparton processes in hadronic collisions*, *JHEP* **07** (2003) 001 [hep-ph/0206293] [INSPIRE].

[25] S. Alioli, P. Nason, C. Oleari and E. Re, *NLO single-top production matched with shower in POWHEG: s- and t-channel contributions*, *JHEP* **09** (2009) 111 [*Erratum ibid.* **02** (2010) 011] [arXiv:0907.4076] [INSPIRE].

[26] E. Re, *Single-top Wt-channel production matched with parton showers using the POWHEG method*, *Eur. Phys. J.* **C 71** (2011) 1547 [arXiv:1009.2450] [INSPIRE].

JHEP11(2017)086

[27] S. Frixione, E. Laenen, P. Motylinski, B.R. Webber and C.D. White, *Single-top hadroproduction in association with a W boson*, *JHEP* **07** (2008) 029 [arXiv:0805.3067] [INSPIRE].

[28] N. Kidonakis, *Next-to-next-to-leading-order collinear and soft gluon corrections for t-channel single top quark production*, *Phys. Rev.* **D 83** (2011) 091503(R) [arXiv:1103.2792] [INSPIRE].

[29] N. Kidonakis, *Two-loop soft anomalous dimensions for single top quark associated production with a W^- or H^-*, *Phys. Rev.* **D 82** (2010) 054018 [arXiv:1005.4451] [INSPIRE].

[30] G. Corcella et al., *HERWIG 6: an event generator for hadron emission reactions with interfering gluons (including supersymmetric processes)*, *JHEP* **01** (2001) 010 [hep-ph/0011363] [INSPIRE].

[31] J.M. Butterworth, J.R. Forshaw and M.H. Seymour, *Multiparton interactions in photoproduction at HERA*, *Z. Phys.* **C 72** (1996) 637 [hep-ph/9601371] [INSPIRE].

[32] ATLAS collaboration, *New ATLAS event generator tunes to 2010 data*, ATL-PHYS-PUB-2011-008 [INSPIRE].

[33] J.M. Campbell, R.K. Ellis and C. Williams, *Vector boson pair production at the LHC*, *JHEP* **07** (2011) 018 [arXiv:1105.0020] [INSPIRE].

[34] P. Nason, *A new method for combining NLO QCD with shower Monte Carlo algorithms*, *JHEP* **11** (2004) 040 [hep-ph/0409146] [INSPIRE].

[35] S. Frixione, P. Nason and C. Oleari, *Matching NLO QCD computations with parton shower simulations: the POWHEG method*, *JHEP* **11** (2007) 070 [arXiv:0709.2092] [INSPIRE].

[36] S. Alioli, P. Nason, C. Oleari and E. Re, *A general framework for implementing NLO calculations in shower Monte Carlo programs: the POWHEG BOX*, *JHEP* **06** (2010) 043 [arXiv:1002.2581] [INSPIRE].

[37] ATLAS collaboration, *The ATLAS Simulation Infrastructure*, *Eur. Phys. J.* **C 70** (2010) 823 [arXiv:1005.4568] [INSPIRE].

[38] GEANT4 collaboration, S. Agostinelli et al., *GEANT4 — a simulation toolkit*, *Nucl. Instrum. Meth.* **A 506** (2003) 250 [INSPIRE].

[39] ATLAS collaboration, *The simulation principle and performance of the ATLAS fast calorimeter simulation FastCaloSim*, ATL-PHYS-PUB-2010-013 [INSPIRE].

[40] ATLAS collaboration, *Luminosity determination in pp collisions at $\sqrt{s} = 8$ TeV using the ATLAS detector at the LHC*, *Eur. Phys. J.* **C 76** (2016) 653 [arXiv:1608.03953] [INSPIRE].

[41] ATLAS collaboration, *Electron reconstruction and identification efficiency measurements with the ATLAS detector using the 2011 LHC proton-proton collision data*, *Eur. Phys. J.* **C 74** (2014) 2941 [arXiv:1404.2240] [INSPIRE].

[42] ATLAS collaboration, *Electron efficiency measurements with the ATLAS detector using 2012 LHC proton-proton collision data*, *Eur. Phys. J.* **C 77** (2017) 195 [arXiv:1612.01456] [INSPIRE].

[43] ATLAS collaboration, *Muon reconstruction efficiency and momentum resolution of the ATLAS experiment in proton-proton collisions at $\sqrt{s} = 7$ TeV in 2010*, *Eur. Phys. J.* **C 74** (2014) 3034 [arXiv:1404.4562] [INSPIRE].

JHEP11(2017)086

[44] ATLAS collaboration, *Measurement of the muon reconstruction performance of the ATLAS detector using 2011 and 2012 LHC proton-proton collision data*, *Eur. Phys. J.* **C 74** (2014) 3130 [arXiv:1407.3935] [INSPIRE].

[45] K. Rehermann and B. Tweedie, *Efficient identification of boosted semileptonic top quarks at the LHC*, *JHEP* **03** (2011) 059 [arXiv:1007.2221] [INSPIRE].

[46] ATLAS collaboration, *Measurement of the photon identification efficiencies with the ATLAS detector using LHC Run-1 data*, *Eur. Phys. J.* **C 76** (2016) 666 [arXiv:1606.01813] [INSPIRE].

[47] W. Lampl et al., *Calorimeter Clustering Algorithms: Description and Performance*, ATL-LARG-PUB-2008-002 [INSPIRE].

[48] ATLAS collaboration, *Electron and photon energy calibration with the ATLAS detector using LHC Run 1 data*, *Eur. Phys. J.* **C 74** (2014) 3071 [arXiv:1407.5063] [INSPIRE].

[49] M. Cacciari, G.P. Salam and G. Soyez, *The anti-k_t jet clustering algorithm*, *JHEP* **04** (2008) 063 [arXiv:0802.1189] [INSPIRE].

[50] ATLAS collaboration, *Topological cell clustering in the ATLAS calorimeters and its performance in LHC Run 1*, *Eur. Phys. J.* **C 77** (2017) 490 [arXiv:1603.02934] [INSPIRE].

[51] ATLAS collaboration, *Jet energy measurement with the ATLAS detector in proton-proton collisions at $\sqrt{s} = 7$ TeV*, *Eur. Phys. J.* **C 73** (2013) 2304 [arXiv:1112.6426] [INSPIRE].

[52] ATLAS collaboration, *Performance of pile-up mitigation techniques for jets in pp collisions at $\sqrt{s} = 8$ TeV using the ATLAS detector*, *Eur. Phys. J.* **C 76** (2016) 581 [arXiv:1510.03823] [INSPIRE].

[53] ATLAS collaboration, *Performance of b-Jet Identification in the ATLAS Experiment*, 2016 *JINST* **11** P04008 [arXiv:1512.01094] [INSPIRE].

[54] ATLAS collaboration, *Calibration of the performance of b-tagging for c and light-flavour jets in the 2012 ATLAS data*, ATLAS-CONF-2014-046 [INSPIRE].

[55] ATLAS collaboration, *Calibration of b-tagging using dileptonic top pair events in a combinatorial likelihood approach with the ATLAS experiment*, ATLAS-CONF-2014-004 [INSPIRE].

[56] ATLAS collaboration, *Performance of algorithms that reconstruct missing transverse momentum in $\sqrt{s} = 8$ TeV proton-proton collisions in the ATLAS detector*, *Eur. Phys. J.* **C 77** (2017) 241 [arXiv:1609.09324] [INSPIRE].

[57] ATLAS collaboration, *Measurement of the top quark-pair production cross section with ATLAS in pp collisions at $\sqrt{s} = 7$ TeV*, *Eur. Phys. J.* **C 71** (2011) 1577 [arXiv:1012.1792] [INSPIRE].

[58] M.J. Oreglia, *A study of the reactions $\psi' \to \gamma\gamma\psi$*, SLAC-R-236 [INSPIRE].

[59] P.-F. Duan, W.-G. Ma, R.-Y. Zhang, L. Han, L. Guo and S.-M. Wang, *QCD corrections to associated production of $t\bar{t}\gamma$ at hadron colliders*, *Phys. Rev.* **D 80** (2009) 014022 [arXiv:0907.1324] [INSPIRE].

[60] W. Verkerke and D. Kirkby, *The RooFit toolkit for data modeling*, [physics/0306116] [INSPIRE].

[61] L. Moneta et al., *The RooStats Project*, PoS(ACAT2010)057 [arXiv:1009.1003] [INSPIRE].

JHEP11(2017)086

[62] F.A. Berends, H. Kuijf, B. Tausk and W.T. Giele, *On the production of a W and jets at hadron colliders*, *Nucl. Phys.* **B 357** (1991) 32 [INSPIRE].

[63] ATLAS collaboration, *Jet energy measurement and its systematic uncertainty in proton-proton collisions at $\sqrt{s} = 7$ TeV with the ATLAS detector*, *Eur. Phys. J.* **C 75** (2015) 17 [arXiv:1406.0076] [INSPIRE].

[64] ATLAS collaboration, *Jet energy resolution in proton-proton collisions at $\sqrt{s} = 7$ TeV recorded in 2010 with the ATLAS detector*, *Eur. Phys. J.* **C 73** (2013) 2306 [arXiv:1210.6210] [INSPIRE].

[65] ATLAS collaboration, *ATLAS Computing Acknowledgements 2016–2017*, ATL-GEN-PUB-2016-002 (2016).

JHEP11(2017)086

The ATLAS collaboration

M. Aaboud[137d], G. Aad[88], B. Abbott[115], O. Abdinov[12,*], B. Abeloos[119], S.H. Abidi[161], O.S. AbouZeid[139], N.L. Abraham[151], H. Abramowicz[155], H. Abreu[154], R. Abreu[118], Y. Abulaiti[148a,148b], B.S. Acharya[167a,167b,a], S. Adachi[157], L. Adamczyk[41a], J. Adelman[110], M. Adersberger[102], T. Adye[133], A.A. Affolder[139], T. Agatonovic-Jovin[14], C. Agheorghiesei[28c], J.A. Aguilar-Saavedra[128a,128f], S.P. Ahlen[24], F. Ahmadov[68,b], G. Aielli[135a,135b], S. Akatsuka[71], H. Akerstedt[148a,148b], T.P.A. Åkesson[84], E. Akilli[52], A.V. Akimov[98], G.L. Alberghi[22a,22b], J. Albert[172], P. Albicocco[50], M.J. Alconada Verzini[74], S.C. Alderweireldt[108], M. Aleksa[32], I.N. Aleksandrov[68], C. Alexa[28b], G. Alexander[155], T. Alexopoulos[10], M. Alhroob[115], B. Ali[130], M. Aliev[76a,76b], G. Alimonti[94a], J. Alison[33], S.P. Alkire[38], B.M.M. Allbrooke[151], B.W. Allen[118], P.P. Allport[19], A. Aloisio[106a,106b], A. Alonso[39], F. Alonso[74], C. Alpigiani[140], A.A. Alshehri[56], M.I. Alstaty[88], B. Alvarez Gonzalez[32], D. Álvarez Piqueras[170], M.G. Alviggi[106a,106b], B.T. Amadio[16], Y. Amaral Coutinho[26a], C. Amelung[25], D. Amidei[92], S.P. Amor Dos Santos[128a,128c], A. Amorim[128a,128b], S. Amoroso[32], G. Amundsen[25], C. Anastopoulos[141], L.S. Ancu[52], N. Andari[19], T. Andeen[11], C.F. Anders[60b], J.K. Anders[77], K.J. Anderson[33], A. Andreazza[94a,94b], V. Andrei[60a], S. Angelidakis[9], I. Angelozzi[109], A. Angerami[38], A.V. Anisenkov[111,c], N. Anjos[13], A. Annovi[126a,126b], C. Antel[60a], M. Antonelli[50], A. Antonov[100,*], D.J. Antrim[166], F. Anulli[134a], M. Aoki[69], L. Aperio Bella[32], G. Arabidze[93], Y. Arai[69], J.P. Araque[128a], V. Araujo Ferraz[26a], A.T.H. Arce[48], R.E. Ardell[80], F.A. Arduh[74], J-F. Arguin[97], S. Argyropoulos[66], M. Arik[20a], A.J. Armbruster[32], L.J. Armitage[79], O. Arnaez[161], H. Arnold[51], M. Arratia[30], O. Arslan[23], A. Artamonov[99], G. Artoni[122], S. Artz[86], S. Asai[157], N. Asbah[45], A. Ashkenazi[155], L. Asquith[151], K. Assamagan[27], R. Astalos[146a], M. Atkinson[169], N.B. Atlay[143], K. Augsten[130], G. Avolio[32], B. Axen[16], M.K. Ayoub[119], G. Azuelos[97,d], A.E. Baas[60a], M.J. Baca[19], H. Bachacou[138], K. Bachas[76a,76b], M. Backes[122], M. Backhaus[32], P. Bagnaia[134a,134b], M. Bahmani[42], H. Bahrasemani[144], J.T. Baines[133], M. Bajic[39], O.K. Baker[179], E.M. Baldin[111,c], P. Balek[175], F. Balli[138], W.K. Balunas[124], E. Banas[42], A. Bandyopadhyay[23], Sw. Banerjee[176,e], A.A.E. Bannoura[178], L. Barak[32], E.L. Barberio[91], D. Barberis[53a,53b], M. Barbero[88], T. Barillari[103], M-S Barisits[32], J.T. Barkeloo[118], T. Barklow[145], N. Barlow[30], S.L. Barnes[36c], B.M. Barnett[133], R.M. Barnett[16], Z. Barnovska-Blenessy[36a], A. Baroncelli[136a], G. Barone[25], A.J. Barr[122], L. Barranco Navarro[170], F. Barreiro[85], J. Barreiro Guimarães da Costa[35a], R. Bartoldus[145], A.E. Barton[75], P. Bartos[146a], A. Basalaev[125], A. Bassalat[119,f], R.L. Bates[56], S.J. Batista[161], J.R. Batley[30], M. Battaglia[139], M. Bauce[134a,134b], F. Bauer[138], H.S. Bawa[145,g], J.B. Beacham[113], M.D. Beattie[75], T. Beau[83], P.H. Beauchemin[165], P. Bechtle[23], H.P. Beck[18,h], H.C. Beck[57], K. Becker[122], M. Becker[86], M. Beckingham[173], C. Becot[112], A.J. Beddall[20e], A. Beddall[20b], V.A. Bednyakov[68], M. Bedognetti[109], C.P. Bee[150], T.A. Beermann[32], M. Begalli[26a], M. Begel[27], J.K. Behr[45], A.S. Bell[81], G. Bella[155], L. Bellagamba[22a], A. Bellerive[31], M. Bellomo[154], K. Belotskiy[100], O. Beltramello[32], N.L. Belyaev[100], O. Benary[155,*], D. Benchekroun[137a], M. Bender[102], K. Bendtz[148a,148b], N. Benekos[10], Y. Benhammou[155], E. Benhar Noccioli[179], J. Benitez[66], D.P. Benjamin[48], M. Benoit[52], J.R. Bensinger[25], S. Bentvelsen[109], L. Beresford[122], M. Beretta[50], D. Berge[109], E. Bergeaas Kuutmann[168], N. Berger[5], J. Beringer[16], S. Berlendis[58], N.R. Bernard[89], G. Bernardi[83], C. Bernius[145], F.U. Bernlochner[23], T. Berry[80], P. Berta[131], C. Bertella[35a], G. Bertoli[148a,148b], F. Bertolucci[126a,126b], I.A. Bertram[75], C. Bertsche[45], D. Bertsche[115], G.J. Besjes[39], O. Bessidskaia Bylund[148a,148b], M. Bessner[45], N. Besson[138], C. Betancourt[51], A. Bethani[87], S. Bethke[103], A.J. Bevan[79], J. Beyer[103], R.M. Bianchi[127], O. Biebel[102], D. Biedermann[17], R. Bielski[87], K. Bierwagen[86], N.V. Biesuz[126a,126b], M. Biglietti[136a], T.R.V. Billoud[97], H. Bilokon[50], M. Bindi[57], A. Bingul[20b], C. Bini[134a,134b], S. Biondi[22a,22b],

JHEP11(2017)086

T. Bisanz[57], C. Bittrich[47], D.M. Bjergaard[48], C.W. Black[152], J.E. Black[145], K.M. Black[24], R.E. Blair[6], T. Blazek[146a], I. Bloch[45], C. Blocker[25], A. Blue[56], W. Blum[86,*], U. Blumenschein[79], S. Blunier[34a], G.J. Bobbink[109], V.S. Bobrovnikov[111,c], S.S. Bocchetta[84], A. Bocci[48], C. Bock[102], M. Boehler[51], D. Boerner[178], D. Bogavac[102], A.G. Bogdanchikov[111], C. Bohm[148a], V. Boisvert[80], P. Bokan[168,i], T. Bold[41a], A.S. Boldyrev[101], A.E. Bolz[60b], M. Bomben[83], M. Bona[79], M. Boonekamp[138], A. Borisov[132], G. Borissov[75], J. Bortfeldt[32], D. Bortoletto[122], V. Bortolotto[62a,62b,62c], D. Boscherini[22a], M. Bosman[13], J.D. Bossio Sola[29], J. Boudreau[127], J. Bouffard[2], E.V. Bouhova-Thacker[75], D. Boumediene[37], C. Bourdarios[119], S.K. Boutle[56], A. Boveia[113], J. Boyd[32], I.R. Boyko[68], J. Bracinik[19], A. Brandt[8], G. Brandt[57], O. Brandt[60a], U. Bratzler[158], B. Brau[89], J.E. Brau[118], W.D. Breaden Madden[56], K. Brendlinger[45], A.J. Brennan[91], L. Brenner[109], R. Brenner[168], S. Bressler[175], D.L. Briglin[19], T.M. Bristow[49], D. Britton[56], D. Britzger[45], F.M. Brochu[30], I. Brock[23], R. Brock[93], G. Brooijmans[38], T. Brooks[80], W.K. Brooks[34b], J. Brosamer[16], E. Brost[110], J.H Broughton[19], P.A. Bruckman de Renstrom[42], D. Bruncko[146b], A. Bruni[22a], G. Bruni[22a], L.S. Bruni[109], BH Brunt[30], M. Bruschi[22a], N. Bruscino[23], P. Bryant[33], L. Bryngemark[45], T. Buanes[15], Q. Buat[144], P. Buchholz[143], A.G. Buckley[56], I.A. Budagov[68], F. Buehrer[51], M.K. Bugge[121], O. Bulekov[100], D. Bullock[8], T.J. Burch[110], S. Burdin[77], C.D. Burgard[51], A.M. Burger[5], B. Burghgrave[110], K. Burka[42], S. Burke[133], I. Burmeister[46], J.T.P. Burr[122], E. Busato[37], D. Büscher[51], V. Büscher[86], P. Bussey[56], J.M. Butler[24], C.M. Buttar[56], J.M. Butterworth[81], P. Butti[32], W. Buttinger[27], A. Buzatu[35c], A.R. Buzykaev[111,c], S. Cabrera Urbán[170], D. Caforio[130], V.M. Cairo[40a,40b], O. Cakir[4a], N. Calace[52], P. Calafiura[16], A. Calandri[88], G. Calderini[83], P. Calfayan[64], G. Callea[40a,40b], L.P. Caloba[26a], S. Calvente Lopez[85], D. Calvet[37], S. Calvet[37], T.P. Calvet[88], R. Camacho Toro[33], S. Camarda[32], P. Camarri[135a,135b], D. Cameron[121], R. Caminal Armadans[169], C. Camincher[58], S. Campana[32], M. Campanelli[81], A. Camplani[94a,94b], A. Campoverde[143], V. Canale[106a,106b], M. Cano Bret[36c], J. Cantero[116], T. Cao[155], M.D.M. Capeans Garrido[32], I. Caprini[28b], M. Caprini[28b], M. Capua[40a,40b], R.M. Carbone[38], R. Cardarelli[135a], F. Cardillo[51], I. Carli[131], T. Carli[32], G. Carlino[106a], B.T. Carlson[127], L. Carminati[94a,94b], R.M.D. Carney[148a,148b], S. Caron[108], E. Carquin[34b], S. Carrá[94a,94b], G.D. Carrillo-Montoya[32], J. Carvalho[128a,128c], D. Casadei[19], M.P. Casado[13,j], M. Casolino[13], D.W. Casper[166], R. Castelijn[109], V. Castillo Gimenez[170], N.F. Castro[128a,k], A. Catinaccio[32], J.R. Catmore[121], A. Cattai[32], J. Caudron[23], V. Cavaliere[169], E. Cavallaro[13], D. Cavalli[94a], M. Cavalli-Sforza[13], V. Cavasinni[126a,126b], E. Celebi[20a], F. Ceradini[136a,136b], L. Cerda Alberich[170], A.S. Cerqueira[26b], A. Cerri[151], L. Cerrito[135a,135b], F. Cerutti[16], A. Cervelli[18], S.A. Cetin[20d], A. Chafaq[137a], D. Chakraborty[110], S.K. Chan[59], W.S. Chan[109], Y.L. Chan[62a], P. Chang[169], J.D. Chapman[30], D.G. Charlton[19], C.C. Chau[161], C.A. Chavez Barajas[151], S. Che[113], S. Cheatham[167a,167c], A. Chegwidden[93], S. Chekanov[6], S.V. Chekulaev[163a], G.A. Chelkov[68,l], M.A. Chelstowska[32], C. Chen[67], H. Chen[27], J. Chen[36a], S. Chen[35b], S. Chen[157], X. Chen[35c,m], Y. Chen[70], H.C. Cheng[92], H.J. Cheng[35a], A. Cheplakov[68], E. Cheremushkina[132], R. Cherkaoui El Moursli[137e], E. Cheu[7], K. Cheung[63], L. Chevalier[138], V. Chiarella[50], G. Chiarelli[126a,126b], G. Chiodini[76a], A.S. Chisholm[32], A. Chitan[28b], Y.H. Chiu[172], M.V. Chizhov[68], K. Choi[64], A.R. Chomont[37], S. Chouridou[156], V. Christodoulou[81], D. Chromek-Burckhart[32], M.C. Chu[62a], J. Chudoba[129], A.J. Chuinard[90], J.J. Chwastowski[42], L. Chytka[117], A.K. Ciftci[4a], D. Cinca[46], V. Cindro[78], I.A. Cioara[23], C. Ciocca[22a,22b], A. Ciocio[16], F. Cirotto[106a,106b], Z.H. Citron[175], M. Citterio[94a], M. Ciubancan[28b], A. Clark[52], B.L. Clark[59], M.R. Clark[38], P.J. Clark[49], R.N. Clarke[16], C. Clement[148a,148b], Y. Coadou[88], M. Cobal[167a,167c], A. Coccaro[52], J. Cochran[67], L. Colasurdo[108], B. Cole[38], A.P. Colijn[109], J. Collot[58], T. Colombo[166], P. Conde Muiño[128a,128b], E. Coniavitis[51], S.H. Connell[147b], I.A. Connelly[87], S. Constantinescu[28b], G. Conti[32], F. Conventi[106a,n], M. Cooke[16], A.M. Cooper-Sarkar[122],

JHEP11(2017)086

F. Cormier[171], K.J.R. Cormier[161], M. Corradi[134a,134b], F. Corriveau[90,o], A. Cortes-Gonzalez[32], G. Cortiana[103], G. Costa[94a], M.J. Costa[170], D. Costanzo[141], G. Cottin[30], G. Cowan[80], B.E. Cox[87], K. Cranmer[112], S.J. Crawley[56], R.A. Creager[124], G. Cree[31], S. Crépé-Renaudin[58], F. Crescioli[83], W.A. Cribbs[148a,148b], M. Cristinziani[23], V. Croft[108], G. Crosetti[40a,40b], A. Cueto[85], T. Cuhadar Donszelmann[141], A.R. Cukierman[145], J. Cummings[179], M. Curatolo[50], J. Cúth[86], P. Czodrowski[32], G. D'amen[22a,22b], S. D'Auria[56], L. D'eramo[83], M. D'Onofrio[77], M.J. Da Cunha Sargedas De Sousa[128a,128b], C. Da Via[87], W. Dabrowski[41a], T. Dado[146a], T. Dai[92], O. Dale[15], F. Dallaire[97], C. Dallapiccola[89], M. Dam[39], J.R. Dandoy[124], M.F. Daneri[29], N.P. Dang[176], A.C. Daniells[19], N.S. Dann[87], M. Danninger[171], M. Dano Hoffmann[138], V. Dao[150], G. Darbo[53a], S. Darmora[8], J. Dassoulas[3], A. Dattagupta[118], T. Daubney[45], W. Davey[23], C. David[45], T. Davidek[131], D.R. Davis[48], P. Davison[81], E. Dawe[91], I. Dawson[141], K. De[8], R. de Asmundis[106a], A. De Benedetti[115], S. De Castro[22a,22b], S. De Cecco[83], N. De Groot[108], P. de Jong[109], H. De la Torre[93], F. De Lorenzi[67], A. De Maria[57], D. De Pedis[134a], A. De Salvo[134a], U. De Sanctis[135a,135b], A. De Santo[151], K. De Vasconcelos Corga[88], J.B. De Vivie De Regie[119], W.J. Dearnaley[75], R. Debbe[27], C. Debenedetti[139], D.V. Dedovich[68], N. Dehghanian[3], I. Deigaard[109], M. Del Gaudio[40a,40b], J. Del Peso[85], D. Delgove[119], F. Deliot[138], C.M. Delitzsch[7], A. Dell'Acqua[32], L. Dell'Asta[24], M. Dell'Orso[126a,126b], M. Della Pietra[106a,106b], D. della Volpe[52], M. Delmastro[5], C. Delporte[119], P.A. Delsart[58], D.A. DeMarco[161], S. Demers[179], M. Demichev[68], A. Demilly[83], S.P. Denisov[132], D. Denysiuk[138], D. Derendarz[42], J.E. Derkaoui[137d], F. Derue[83], P. Dervan[77], K. Desch[23], C. Deterre[45], K. Dette[46], M.R. Devesa[29], P.O. Deviveiros[32], A. Dewhurst[133], S. Dhaliwal[25], F.A. Di Bello[52], A. Di Ciaccio[135a,135b], L. Di Ciaccio[5], W.K. Di Clemente[124], C. Di Donato[106a,106b], A. Di Girolamo[32], B. Di Girolamo[32], B. Di Micco[136a,136b], R. Di Nardo[32], K.F. Di Petrillo[59], A. Di Simone[51], R. Di Sipio[161], D. Di Valentino[31], C. Diaconu[88], M. Diamond[161], F.A. Dias[39], M.A. Diaz[34a], E.B. Diehl[92], J. Dietrich[17], S. Díez Cornell[45], A. Dimitrievska[14], J. Dingfelder[23], P. Dita[28b], S. Dita[28b], F. Dittus[32], F. Djama[88], T. Djobava[54b], J.I. Djuvsland[60a], M.A.B. do Vale[26c], D. Dobos[32], M. Dobre[28b], C. Doglioni[84], J. Dolejsi[131], Z. Dolezal[131], M. Donadelli[26d], S. Donati[126a,126b], P. Dondero[123a,123b], J. Donini[37], J. Dopke[133], A. Doria[106a], M.T. Dova[74], A.T. Doyle[56], E. Drechsler[57], M. Dris[10], Y. Du[36b], J. Duarte-Campderros[155], A. Dubreuil[52], E. Duchovni[175], G. Duckeck[102], A. Ducourthial[83], O.A. Ducu[97,p], D. Duda[109], A. Dudarev[32], A.Chr. Dudder[86], E.M. Duffield[16], L. Duflot[119], M. Dührssen[32], M. Dumancic[175], A.E. Dumitriu[28b], A.K. Duncan[56], M. Dunford[60a], H. Duran Yildiz[4a], M. Düren[55], A. Durglishvili[54b], D. Duschinger[47], B. Dutta[45], M. Dyndal[45], B.S. Dziedzic[42], C. Eckardt[45], K.M. Ecker[103], R.C. Edgar[92], T. Eifert[32], G. Eigen[15], K. Einsweiler[16], T. Ekelof[168], M. El Kacimi[137c], R. El Kosseifi[88], V. Ellajosyula[88], M. Ellert[168], S. Elles[5], F. Ellinghaus[178], A.A. Elliot[172], N. Ellis[32], J. Elmsheuser[27], M. Elsing[32], D. Emeliyanov[133], Y. Enari[157], O.C. Endner[86], J.S. Ennis[173], J. Erdmann[46], A. Ereditato[18], M. Ernst[27], S. Errede[169], M. Escalier[119], C. Escobar[170], B. Esposito[50], O. Estrada Pastor[170], A.I. Etienvre[138], E. Etzion[155], H. Evans[64], A. Ezhilov[125], M. Ezzi[137e], F. Fabbri[22a,22b], L. Fabbri[22a,22b], V. Fabiani[108], G. Facini[81], R.M. Fakhrutdinov[132], S. Falciano[134a], R.J. Falla[81], J. Faltova[32], Y. Fang[35a], M. Fanti[94a,94b], A. Farbin[8], A. Farilla[136a], C. Farina[127], E.M. Farina[123a,123b], T. Farooque[93], S. Farrell[16], S.M. Farrington[173], P. Farthouat[32], F. Fassi[137e], P. Fassnacht[32], D. Fassouliotis[9], M. Faucci Giannelli[80], A. Favareto[53a,53b], W.J. Fawcett[122], L. Fayard[119], O.L. Fedin[125,q], W. Fedorko[171], S. Feigl[121], L. Feligioni[88], C. Feng[36b], E.J. Feng[32], H. Feng[92], M.J. Fenton[56], A.B. Fenyuk[132], L. Feremenga[8], P. Fernandez Martinez[170], S. Fernandez Perez[13], J. Ferrando[45], A. Ferrari[168], P. Ferrari[109], R. Ferrari[123a], D.E. Ferreira de Lima[60b], A. Ferrer[170], D. Ferrere[52], C. Ferretti[92], F. Fiedler[86], A. Filipčič[78], M. Filipuzzi[45], F. Filthaut[108], M. Fincke-Keeler[172], K.D. Finelli[152], M.C.N. Fiolhais[128a,128c,r], L. Fiorini[170], A. Fischer[2], C. Fischer[13], J. Fischer[178], W.C. Fisher[93], N. Flaschel[45], I. Fleck[143],

JHEP11(2017)086

P. Fleischmann[92], R.R.M. Fletcher[124], T. Flick[178], B.M. Flierl[102], L.R. Flores Castillo[62a], M.J. Flowerdew[103], G.T. Forcolin[87], A. Formica[138], F.A. Förster[13], A. Forti[87], A.G. Foster[19], D. Fournier[119], H. Fox[75], S. Fracchia[141], P. Francavilla[83], M. Franchini[22a,22b], S. Franchino[60a], D. Francis[32], L. Franconi[121], M. Franklin[59], M. Frate[166], M. Fraternali[123a,123b], D. Freeborn[81], S.M. Fressard-Batraneanu[32], B. Freund[97], D. Froidevaux[32], J.A. Frost[122], C. Fukunaga[158], T. Fusayasu[104], J. Fuster[170], C. Gabaldon[58], O. Gabizon[154], A. Gabrielli[22a,22b], A. Gabrielli[16], G.P. Gach[41a], S. Gadatsch[32], S. Gadomski[80], G. Gagliardi[53a,53b], L.G. Gagnon[97], C. Galea[108], B. Galhardo[128a,128c], E.J. Gallas[122], B.J. Gallop[133], P. Gallus[130], G. Galster[39], K.K. Gan[113], S. Ganguly[37], Y. Gao[77], Y.S. Gao[145,g], F.M. Garay Walls[49], C. García[170], J.E. García Navarro[170], J.A. García Pascual[35a], M. Garcia-Sciveres[16], R.W. Gardner[33], N. Garelli[145], V. Garonne[121], A. Gascon Bravo[45], K. Gasnikova[45], C. Gatti[50], A. Gaudiello[53a,53b], G. Gaudio[123a], I.L. Gavrilenko[98], C. Gay[171], G. Gaycken[23], E.N. Gazis[10], C.N.P. Gee[133], J. Geisen[57], M. Geisen[86], M.P. Geisler[60a], K. Gellerstedt[148a,148b], C. Gemme[53a], M.H. Genest[58], C. Geng[92], S. Gentile[134a,134b], C. Gentsos[156], S. George[80], D. Gerbaudo[13], A. Gershon[155], G. Geßner[46], S. Ghasemi[143], M. Ghneimat[23], B. Giacobbe[22a], S. Giagu[134a,134b], N. Giangiacomi[22a,22b], P. Giannetti[126a,126b], S.M. Gibson[80], M. Gignac[171], M. Gilchriese[16], D. Gillberg[31], G. Gilles[178], D.M. Gingrich[3,d], N. Giokaris[9,*], M.P. Giordani[167a,167c], F.M. Giorgi[22a], P.F. Giraud[138], P. Giromini[59], G. Giugliarelli[167a,167c], D. Giugni[94a], F. Giuli[122], C. Giuliani[103], M. Giulini[60b], B.K. Gjelsten[121], S. Gkaitatzis[156], I. Gkialas[9,s], E.L. Gkougkousis[139], P. Gkountoumis[10], L.K. Gladilin[101], C. Glasman[85], J. Glatzer[13], P.C.F. Glaysher[45], A. Glazov[45], M. Goblirsch-Kolb[25], J. Godlewski[42], S. Goldfarb[91], T. Golling[52], D. Golubkov[132], A. Gomes[128a,128b,128d], R. Gonçalo[128a], R. Goncalves Gama[26a], J. Goncalves Pinto Firmino Da Costa[138], G. Gonella[51], L. Gonella[19], A. Gongadze[68], S. González de la Hoz[170], S. Gonzalez-Sevilla[52], L. Goossens[32], P.A. Gorbounov[99], H.A. Gordon[27], I. Gorelov[107], B. Gorini[32], E. Gorini[76a,76b], A. Gorišek[78], A.T. Goshaw[48], C. Gössling[46], M.I. Gostkin[68], C.A. Gottardo[23], C.R. Goudet[119], D. Goujdami[137c], A.G. Goussiou[140], N. Govender[147b,t], E. Gozani[154], L. Graber[57], I. Grabowska-Bold[41a], P.O.J. Gradin[168], J. Gramling[166], E. Gramstad[121], S. Grancagnolo[17], V. Gratchev[125], P.M. Gravila[28f], C. Gray[56], H.M. Gray[16], Z.D. Greenwood[82,u], C. Grefe[23], K. Gregersen[81], I.M. Gregor[45], P. Grenier[145], K. Grevtsov[5], J. Griffiths[8], A.A. Grillo[139], K. Grimm[75], S. Grinstein[13,v], Ph. Gris[37], J.-F. Grivaz[119], S. Groh[86], E. Gross[175], J. Grosse-Knetter[57], G.C. Grossi[82], Z.J. Grout[81], A. Grummer[107], L. Guan[92], W. Guan[176], J. Guenther[65], F. Guescini[163a], D. Guest[166], O. Gueta[155], B. Gui[113], E. Guido[53a,53b], T. Guillemin[5], S. Guindon[2], U. Gul[56], C. Gumpert[32], J. Guo[36c], W. Guo[92], Y. Guo[36a], R. Gupta[43], S. Gupta[122], G. Gustavino[134a,134b], P. Gutierrez[115], N.G. Gutierrez Ortiz[81], C. Gutschow[81], C. Guyot[138], M.P. Guzik[41a], C. Gwenlan[122], C.B. Gwilliam[77], A. Haas[112], C. Haber[16], H.K. Hadavand[8], N. Haddad[137e], A. Hadef[88], S. Hageböck[23], M. Hagihara[164], H. Hakobyan[180,*], M. Haleem[45], J. Haley[116], G. Halladjian[93], G.D. Hallewell[88], K. Hamacher[178], P. Hamal[117], K. Hamano[172], A. Hamilton[147a], G.N. Hamity[141], P.G. Hamnett[45], L. Han[36a], S. Han[35a], K. Hanagaki[69,w], K. Hanawa[157], M. Hance[139], B. Haney[124], P. Hanke[60a], J.B. Hansen[39], J.D. Hansen[39], M.C. Hansen[23], P.H. Hansen[39], K. Hara[164], A.S. Hard[176], T. Harenberg[178], F. Hariri[119], S. Harkusha[95], R.D. Harrington[49], P.F. Harrison[173], N.M. Hartmann[102], M. Hasegawa[70], Y. Hasegawa[142], A. Hasib[49], S. Hassani[138], S. Haug[18], R. Hauser[93], L. Hauswald[47], L.B. Havener[38], M. Havranek[130], C.M. Hawkes[19], R.J. Hawkings[32], D. Hayakawa[159], D. Hayden[93], C.P. Hays[122], J.M. Hays[79], H.S. Hayward[77], S.J. Haywood[133], S.J. Head[19], T. Heck[86], V. Hedberg[84], L. Heelan[8], S. Heer[23], K.K. Heidegger[51], S. Heim[45], T. Heim[16], B. Heinemann[45,x], J.J. Heinrich[102], L. Heinrich[112], C. Heinz[55], J. Hejbal[129], L. Helary[32], A. Held[171], S. Hellman[148a,148b], C. Helsens[32], R.C.W. Henderson[75], Y. Heng[176], S. Henkelmann[171], A.M. Henriques Correia[32], S. Henrot-Versille[119], G.H. Herbert[17],

JHEP11(2017)086

H. Herde[25], V. Herget[177], Y. Hernández Jiménez[147c], H. Herr[86], G. Herten[51], R. Hertenberger[102], L. Hervas[32], T.C. Herwig[124], G.G. Hesketh[81], N.P. Hessey[163a], J.W. Hetherly[43], S. Higashino[69], E. Higón-Rodriguez[170], K. Hildebrand[33], E. Hill[172], J.C. Hill[30], K.H. Hiller[45], S.J. Hillier[19], M. Hils[47], I. Hinchliffe[16], M. Hirose[51], D. Hirschbuehl[178], B. Hiti[78], O. Hladik[129], X. Hoad[49], J. Hobbs[150], N. Hod[163a], M.C. Hodgkinson[141], P. Hodgson[141], A. Hoecker[32], M.R. Hoeferkamp[107], F. Hoenig[102], D. Hohn[23], T.R. Holmes[33], M. Homann[46], S. Honda[164], T. Honda[69], T.M. Hong[127], B.H. Hooberman[169], W.H. Hopkins[118], Y. Horii[105], A.J. Horton[144], J-Y. Hostachy[58], S. Hou[153], A. Hoummada[137a], J. Howarth[87], J. Hoya[74], M. Hrabovsky[117], J. Hrdinka[32], I. Hristova[17], J. Hrivnac[119], T. Hryn'ova[5], A. Hrynevich[96], P.J. Hsu[63], S.-C. Hsu[140], Q. Hu[36a], S. Hu[36c], Y. Huang[35a], Z. Hubacek[130], F. Hubaut[88], F. Huegging[23], T.B. Huffman[122], E.W. Hughes[38], G. Hughes[75], M. Huhtinen[32], P. Huo[150], N. Huseynov[68,b], J. Huston[93], J. Huth[59], G. Iacobucci[52], G. Iakovidis[27], I. Ibragimov[143], L. Iconomidou-Fayard[119], Z. Idrissi[137e], P. Iengo[32], O. Igonkina[109,y], T. Iizawa[174], Y. Ikegami[69], M. Ikeno[69], Y. Ilchenko[11,z], D. Iliadis[156], N. Ilic[145], G. Introzzi[123a,123b], P. Ioannou[9,*], M. Iodice[136a], K. Iordanidou[38], V. Ippolito[59], M.F. Isacson[168], N. Ishijima[120], M. Ishino[157], M. Ishitsuka[159], C. Issever[122], S. Istin[20a], F. Ito[164], J.M. Iturbe Ponce[62a], R. Iuppa[162a,162b], H. Iwasaki[69], J.M. Izen[44], V. Izzo[106a], S. Jabbar[3], P. Jackson[1], R.M. Jacobs[23], V. Jain[2], K.B. Jakobi[86], K. Jakobs[51], S. Jakobsen[65], T. Jakoubek[129], D.O. Jamin[116], D.K. Jana[82], R. Jansky[52], J. Janssen[23], M. Janus[57], P.A. Janus[41a], G. Jarlskog[84], N. Javadov[68,b], T. Javůrek[51], M. Javurkova[51], F. Jeanneau[138], L. Jeanty[16], J. Jejelava[54a,aa], A. Jelinskas[173], P. Jenni[51,ab], C. Jeske[173], S. Jézéquel[5], H. Ji[176], J. Jia[150], H. Jiang[67], Y. Jiang[36a], Z. Jiang[145], S. Jiggins[81], J. Jimenez Pena[170], S. Jin[35a], A. Jinaru[28b], O. Jinnouchi[159], H. Jivan[147c], P. Johansson[141], K.A. Johns[7], C.A. Johnson[64], W.J. Johnson[140], K. Jon-And[148a,148b], R.W.L. Jones[75], S.D. Jones[151], S. Jones[7], T.J. Jones[77], J. Jongmanns[60a], P.M. Jorge[128a,128b], J. Jovicevic[163a], X. Ju[176], A. Juste Rozas[13,v], M.K. Köhler[175], A. Kaczmarska[42], M. Kado[119], H. Kagan[113], M. Kagan[145], S.J. Kahn[88], T. Kaji[174], E. Kajomovitz[48], C.W. Kalderon[84], A. Kaluza[86], S. Kama[43], A. Kamenshchikov[132], N. Kanaya[157], L. Kanjir[78], V.A. Kantserov[100], J. Kanzaki[69], B. Kaplan[112], L.S. Kaplan[176], D. Kar[147c], K. Karakostas[10], N. Karastathis[10], M.J. Kareem[57], E. Karentzos[10], S.N. Karpov[68], Z.M. Karpova[68], K. Karthik[112], V. Kartvelishvili[75], A.N. Karyukhin[132], K. Kasahara[164], L. Kashif[176], R.D. Kass[113], A. Kastanas[149], Y. Kataoka[157], C. Kato[157], A. Katre[52], J. Katzy[45], K. Kawade[70], K. Kawagoe[73], T. Kawamoto[157], G. Kawamura[57], E.F. Kay[77], V.F. Kazanin[111,c], R. Keeler[172], R. Kehoe[43], J.S. Keller[31], J.J. Kempster[80], J Kendrick[19], H. Keoshkerian[161], O. Kepka[129], B.P. Kerševan[78], S. Kersten[178], R.A. Keyes[90], M. Khader[169], F. Khalil-zada[12], A. Khanov[116], A.G. Kharlamov[111,c], T. Kharlamova[111,c], A. Khodinov[160], T.J. Khoo[52], V. Khovanskiy[99,*], E. Khramov[68], J. Khubua[54b,ac], S. Kido[70], C.R. Kilby[80], H.Y. Kim[8], S.H. Kim[164], Y.K. Kim[33], N. Kimura[156], O.M. Kind[17], B.T. King[77], D. Kirchmeier[47], J. Kirk[133], A.E. Kiryunin[103], T. Kishimoto[157], D. Kisielewska[41a], V. Kitali[45], K. Kiuchi[164], O. Kivernyk[5], E. Kladiva[146b], T. Klapdor-Kleingrothaus[51], M.H. Klein[38], M. Klein[77], U. Klein[77], K. Kleinknecht[86], P. Klimek[110], A. Klimentov[27], R. Klingenberg[46], T. Klingl[23], T. Klioutchnikova[32], E.-E. Kluge[60a], P. Kluit[109], S. Kluth[103], E. Kneringer[65], E.B.F.G. Knoops[88], A. Knue[103], A. Kobayashi[157], D. Kobayashi[159], T. Kobayashi[157], M. Kobel[47], M. Kocian[145], P. Kodys[131], T. Koffas[31], E. Koffeman[109], N.M. Köhler[103], T. Koi[145], M. Kolb[60b], I. Koletsou[5], A.A. Komar[98,*], Y. Komori[157], T. Kondo[69], N. Kondrashova[36c], K. Köneke[51], A.C. König[108], T. Kono[69,ad], R. Konoplich[112,ae], N. Konstantinidis[81], R. Kopeliansky[64], S. Koperny[41a], A.K. Kopp[51], K. Korcyl[42], K. Kordas[156], A. Korn[81], A.A. Korol[111,c], I. Korolkov[13], E.V. Korolkova[141], O. Kortner[103], S. Kortner[103], T. Kosek[131], V.V. Kostyukhin[23], A. Kotwal[48], A. Koulouris[10], A. Kourkoumeli-Charalampidi[123a,123b], C. Kourkoumelis[9], E. Kourlitis[141], V. Kouskoura[27], A.B. Kowalewska[42], R. Kowalewski[172], T.Z. Kowalski[41a], C. Kozakai[157],

JHEP11(2017)086

W. Kozanecki[138], A.S. Kozhin[132], V.A. Kramarenko[101], G. Kramberger[78], D. Krasnopevtsev[100], M.W. Krasny[83], A. Krasznahorkay[32], D. Krauss[103], J.A. Kremer[41a], J. Kretzschmar[77], K. Kreutzfeldt[55], P. Krieger[161], K. Krizka[33], K. Kroeninger[46], H. Kroha[103], J. Kroll[129], J. Kroll[124], J. Kroseberg[23], J. Krstic[14], U. Kruchonak[68], H. Krüger[23], N. Krumnack[67], M.C. Kruse[48], T. Kubota[91], H. Kucuk[81], S. Kuday[4b], J.T. Kuechler[178], S. Kuehn[32], A. Kugel[60a], F. Kuger[177], T. Kuhl[45], V. Kukhtin[68], R. Kukla[88], Y. Kulchitsky[95], S. Kuleshov[34b], Y.P. Kulinich[169], M. Kuna[134a,134b], T. Kunigo[71], A. Kupco[129], T. Kupfer[46], O. Kuprash[155], H. Kurashige[70], L.L. Kurchaninov[163a], Y.A. Kurochkin[95], M.G. Kurth[35a], V. Kus[129], E.S. Kuwertz[172], M. Kuze[159], J. Kvita[117], T. Kwan[172], D. Kyriazopoulos[141], A. La Rosa[103], J.L. La Rosa Navarro[26d], L. La Rotonda[40a,40b], F. La Ruffa[40a,40b], C. Lacasta[170], F. Lacava[134a,134b], J. Lacey[45], H. Lacker[17], D. Lacour[83], E. Ladygin[68], R. Lafaye[5], B. Laforge[83], T. Lagouri[179], S. Lai[57], S. Lammers[64], W. Lampl[7], E. Lançon[27], U. Landgraf[51], M.P.J. Landon[79], M.C. Lanfermann[52], V.S. Lang[60a], J.C. Lange[13], R.J. Langenberg[32], A.J. Lankford[166], F. Lanni[27], K. Lantzsch[23], A. Lanza[123a], A. Lapertosa[53a,53b], S. Laplace[83], J.F. Laporte[138], T. Lari[94a], F. Lasagni Manghi[22a,22b], M. Lassnig[32], P. Laurelli[50], W. Lavrijsen[16], A.T. Law[139], P. Laycock[77], T. Lazovich[59], M. Lazzaroni[94a,94b], B. Le[91], O. Le Dortz[83], E. Le Guirriec[88], E.P. Le Quilleuc[138], M. LeBlanc[172], T. LeCompte[6], F. Ledroit-Guillon[58], C.A. Lee[27], G.R. Lee[133,af], S.C. Lee[153], L. Lee[59], B. Lefebvre[90], G. Lefebvre[83], M. Lefebvre[172], F. Legger[102], C. Leggett[16], G. Lehmann Miotto[32], X. Lei[7], W.A. Leight[45], M.A.L. Leite[26d], R. Leitner[131], D. Lellouch[175], B. Lemmer[57], K.J.C. Leney[81], T. Lenz[23], B. Lenzi[32], R. Leone[7], S. Leone[126a,126b], C. Leonidopoulos[49], G. Lerner[151], C. Leroy[97], A.A.J. Lesage[138], C.G. Lester[30], M. Levchenko[125], J. Levêque[5], D. Levin[92], L.J. Levinson[175], M. Levy[19], D. Lewis[79], B. Li[36a,ag], Changqiao Li[36a], H. Li[150], L. Li[36c], Q. Li[35a], S. Li[48], X. Li[36c], Y. Li[143], Z. Liang[35a], B. Liberti[135a], A. Liblong[161], K. Lie[62c], J. Liebal[23], W. Liebig[15], A. Limosani[152], S.C. Lin[182], T.H. Lin[86], B.E. Lindquist[150], A.E. Lionti[52], E. Lipeles[124], A. Lipniacka[15], M. Lisovyi[60b], T.M. Liss[169,ah], A. Lister[171], A.M. Litke[139], B. Liu[153,ai], H. Liu[92], H. Liu[27], J.K.K. Liu[122], J. Liu[36b], J.B. Liu[36a], K. Liu[88], L. Liu[169], M. Liu[36a], Y.L. Liu[36a], Y. Liu[36a], M. Livan[123a,123b], A. Lleres[58], J. Llorente Merino[35a], S.L. Lloyd[79], C.Y. Lo[62b], F. Lo Sterzo[153], E.M. Lobodzinska[45], P. Loch[7], F.K. Loebinger[87], A. Loesle[51], K.M. Loew[25], A. Loginov[179,*], T. Lohse[17], K. Lohwasser[141], M. Lokajicek[129], B.A. Long[24], J.D. Long[169], R.E. Long[75], L. Longo[76a,76b], K.A. Looper[113], J.A. Lopez[34b], D. Lopez Mateos[59], I. Lopez Paz[13], A. Lopez Solis[83], J. Lorenz[102], N. Lorenzo Martinez[5], M. Losada[21], P.J. Lösel[102], X. Lou[35a], A. Lounis[119], J. Love[6], P.A. Love[75], H. Lu[62a], N. Lu[92], Y.J. Lu[63], H.J. Lubatti[140], C. Luci[134a,134b], A. Lucotte[58], C. Luedtke[51], F. Luehring[64], W. Lukas[65], L. Luminari[134a], O. Lundberg[148a,148b], B. Lund-Jensen[149], M.S. Lutz[89], P.M. Luzi[83], D. Lynn[27], R. Lysak[129], E. Lytken[84], F. Lyu[35a], V. Lyubushkin[68], H. Ma[27], L.L. Ma[36b], Y. Ma[36b], G. Maccarrone[50], A. Macchiolo[103], C.M. Macdonald[141], B. Maček[78], J. Machado Miguens[124,128b], D. Madaffari[170], R. Madar[37], W.F. Mader[47], A. Madsen[45], J. Maeda[70], S. Maeland[15], T. Maeno[27], A.S. Maevskiy[101], V. Magerl[51], J. Mahlstedt[109], C. Maiani[119], C. Maidantchik[26a], A.A. Maier[103], T. Maier[102], A. Maio[128a,128b,128d], O. Majersky[146a], S. Majewski[118], Y. Makida[69], N. Makovec[119], B. Malaescu[83], Pa. Malecki[42], V.P. Maleev[125], F. Malek[58], U. Mallik[66], D. Malon[6], C. Malone[30], S. Maltezos[10], S. Malyukov[32], J. Mamuzic[170], G. Mancini[50], I. Mandić[78], J. Maneira[128a,128b], L. Manhaes de Andrade Filho[26b], J. Manjarres Ramos[47], K.H. Mankinen[84], A. Mann[102], A. Manousos[32], B. Mansoulie[138], J.D. Mansour[35a], R. Mantifel[90], M. Mantoani[57], S. Manzoni[94a,94b], L. Mapelli[32], G. Marceca[29], L. March[52], L. Marchese[122], G. Marchiori[83], M. Marcisovsky[129], M. Marjanovic[37], D.E. Marley[92], F. Marroquim[26a], S.P. Marsden[87], Z. Marshall[16], M.U.F Martensson[168], S. Marti-Garcia[170], C.B. Martin[113], T.A. Martin[173], V.J. Martin[49], B. Martin dit Latour[15], M. Martinez[13,v], V.I. Martinez Outschoorn[169], S. Martin-Haugh[133], V.S. Martoiu[28b], A.C. Martyniuk[81],

JHEP11(2017)086

A. Marzin[32], L. Masetti[86], T. Mashimo[157], R. Mashinistov[98], J. Masik[87], A.L. Maslennikov[111,c], L. Massa[135a,135b], P. Mastrandrea[5], A. Mastroberardino[40a,40b], T. Masubuchi[157], P. Mättig[178], J. Maurer[28b], S.J. Maxfield[77], D.A. Maximov[111,c], R. Mazini[153], I. Maznas[156], S.M. Mazza[94a,94b], N.C. Mc Fadden[107], G. Mc Goldrick[161], S.P. Mc Kee[92], A. McCarn[92], R.L. McCarthy[150], T.G. McCarthy[103], L.I. McClymont[81], E.F. McDonald[91], J.A. Mcfayden[81], G. Mchedlidze[57], S.J. McMahon[133], P.C. McNamara[91], R.A. McPherson[172,o], S. Meehan[140], T.J. Megy[51], S. Mehlhase[102], A. Mehta[77], T. Meideck[58], K. Meier[60a], B. Meirose[44], D. Melini[170,aj], B.R. Mellado Garcia[147c], J.D. Mellenthin[57], M. Melo[146a], F. Meloni[18], A. Melzer[23], S.B. Menary[87], L. Meng[77], X.T. Meng[92], A. Mengarelli[22a,22b], S. Menke[103], E. Meoni[40a,40b], S. Mergelmeyer[17], P. Mermod[52], L. Merola[106a,106b], C. Meroni[94a], F.S. Merritt[33], A. Messina[134a,134b], J. Metcalfe[6], A.S. Mete[166], C. Meyer[124], J-P. Meyer[138], J. Meyer[109], H. Meyer Zu Theenhausen[60a], F. Miano[151], R.P. Middleton[133], S. Miglioranzi[53a,53b], L. Mijović[49], G. Mikenberg[175], M. Mikestikova[129], M. Mikuž[78], M. Milesi[91], A. Milic[161], D.W. Miller[33], C. Mills[49], A. Milov[175], D.A. Milstead[148a,148b], A.A. Minaenko[132], Y. Minami[157], I.A. Minashvili[68], A.I. Mincer[112], B. Mindur[41a], M. Mineev[68], Y. Minegishi[157], Y. Ming[176], L.M. Mir[13], K.P. Mistry[124], T. Mitani[174], J. Mitrevski[102], V.A. Mitsou[170], A. Miucci[18], P.S. Miyagawa[141], A. Mizukami[69], J.U. Mjörnmark[84], T. Mkrtchyan[180], M. Mlynarikova[131], T. Moa[148a,148b], K. Mochizuki[97], P. Mogg[51], S. Mohapatra[38], S. Molander[148a,148b], R. Moles-Valls[23], R. Monden[71], M.C. Mondragon[93], K. Mönig[45], J. Monk[39], E. Monnier[88], A. Montalbano[150], J. Montejo Berlingen[32], F. Monticelli[74], S. Monzani[94a,94b], R.W. Moore[3], N. Morange[119], D. Moreno[21], M. Moreno Llácer[32], P. Morettini[53a], S. Morgenstern[32], D. Mori[144], T. Mori[157], M. Morii[59], M. Morinaga[157], V. Morisbak[121], A.K. Morley[32], G. Mornacchi[32], J.D. Morris[79], L. Morvaj[150], P. Moschovakos[10], M. Mosidze[54b], H.J. Moss[141], J. Moss[145,ak], K. Motohashi[159], R. Mount[145], E. Mountricha[27], E.J.W. Moyse[89], S. Muanza[88], F. Mueller[103], J. Mueller[127], R.S.P. Mueller[102], D. Muenstermann[75], P. Mullen[56], G.A. Mullier[18], F.J. Munoz Sanchez[87], W.J. Murray[173,133], H. Musheghyan[32], M. Muškinja[78], A.G. Myagkov[132,al], M. Myska[130], B.P. Nachman[16], O. Nackenhorst[52], K. Nagai[122], R. Nagai[69,ad], K. Nagano[69], Y. Nagasaka[61], K. Nagata[164], M. Nagel[51], E. Nagy[88], A.M. Nairz[32], Y. Nakahama[105], K. Nakamura[69], T. Nakamura[157], I. Nakano[114], R.F. Naranjo Garcia[45], R. Narayan[11], D.I. Narrias Villar[60a], I. Naryshkin[125], T. Naumann[45], G. Navarro[21], R. Nayyar[7], H.A. Neal[92], P.Yu. Nechaeva[98], T.J. Neep[138], A. Negri[123a,123b], M. Negrini[22a], S. Nektarijevic[108], C. Nellist[119], A. Nelson[166], M.E. Nelson[122], S. Nemecek[129], P. Nemethy[112], M. Nessi[32,am], M.S. Neubauer[169], M. Neumann[178], P.R. Newman[19], T.Y. Ng[62c], T. Nguyen Manh[97], R.B. Nickerson[122], R. Nicolaidou[138], J. Nielsen[139], V. Nikolaenko[132,al], I. Nikolic-Audit[83], K. Nikolopoulos[19], J.K. Nilsen[121], P. Nilsson[27], Y. Ninomiya[157], A. Nisati[134a], N. Nishu[35c], R. Nisius[103], I. Nitsche[46], T. Nitta[174], T. Nobe[157], Y. Noguchi[71], M. Nomachi[120], I. Nomidis[31], M.A. Nomura[27], T. Nooney[79], M. Nordberg[32], N. Norjoharuddeen[122], O. Novgorodova[47], S. Nowak[103], M. Nozaki[69], L. Nozka[117], K. Ntekas[166], E. Nurse[81], F. Nuti[91], K. O'connor[25], D.C. O'Neil[144], A.A. O'Rourke[45], V. O'Shea[56], F.G. Oakham[31,d], H. Oberlack[103], T. Obermann[23], J. Ocariz[83], A. Ochi[70], I. Ochoa[38], J.P. Ochoa-Ricoux[34a], S. Oda[73], S. Odaka[69], A. Oh[87], S.H. Oh[48], C.C. Ohm[16], H. Ohman[168], H. Oide[53a,53b], H. Okawa[164], Y. Okumura[157], T. Okuyama[69], A. Olariu[28b], L.F. Oleiro Seabra[128a], S.A. Olivares Pino[49], D. Oliveira Damazio[27], A. Olszewski[42], J. Olszowska[42], A. Onofre[128a,128e], K. Onogi[105], P.U.E. Onyisi[11,z], H. Oppen[121], M.J. Oreglia[33], Y. Oren[155], D. Orestano[136a,136b], N. Orlando[62b], R.S. Orr[161], B. Osculati[53a,53b,*], R. Ospanov[36a], G. Otero y Garzon[29], H. Otono[73], M. Ouchrif[137d], F. Ould-Saada[121], A. Ouraou[138], K.P. Oussoren[109], Q. Ouyang[35a], M. Owen[56], R.E. Owen[19], V.E. Ozcan[20a], N. Ozturk[8], K. Pachal[144], A. Pacheco Pages[13], L. Pacheco Rodriguez[138], C. Padilla Aranda[13], S. Pagan Griso[16], M. Paganini[179], F. Paige[27], G. Palacino[64], S. Palazzo[40a,40b], S. Palestini[32],

JHEP11(2017)086

M. Palka[41b], D. Pallin[37], E.St. Panagiotopoulou[10], I. Panagoulias[10], C.E. Pandini[126a,126b], J.G. Panduro Vazquez[80], P. Pani[32], S. Panitkin[27], D. Pantea[28b], L. Paolozzi[52], Th.D. Papadopoulou[10], K. Papageorgiou[9,s], A. Paramonov[6], D. Paredes Hernandez[179], A.J. Parker[75], M.A. Parker[30], K.A. Parker[45], F. Parodi[53a,53b], J.A. Parsons[38], U. Parzefall[51], V.R. Pascuzzi[161], J.M. Pasner[139], E. Pasqualucci[134a], S. Passaggio[53a], Fr. Pastore[80], S. Pataraia[86], J.R. Pater[87], T. Pauly[32], B. Pearson[103], S. Pedraza Lopez[170], R. Pedro[128a,128b], S.V. Peleganchuk[111,c], O. Penc[129], C. Peng[35a], H. Peng[36a], J. Penwell[64], B.S. Peralva[26b], M.M. Perego[138], D.V. Perepelitsa[27], F. Peri[17], L. Perini[94a,94b], H. Pernegger[32], S. Perrella[106a,106b], R. Peschke[45], V.D. Peshekhonov[68,*], K. Peters[45], R.F.Y. Peters[87], B.A. Petersen[32], T.C. Petersen[39], E. Petit[58], A. Petridis[1], C. Petridou[156], P. Petroff[119], E. Petrolo[134a], M. Petrov[122], F. Petrucci[136a,136b], N.E. Pettersson[89], A. Peyaud[138], R. Pezoa[34b], F.H. Phillips[93], P.W. Phillips[133], G. Piacquadio[150], E. Pianori[173], A. Picazio[89], E. Piccaro[79], M.A. Pickering[122], R. Piegaia[29], J.E. Pilcher[33], A.D. Pilkington[87], A.W.J. Pin[87], M. Pinamonti[135a,135b], J.L. Pinfold[3], H. Pirumov[45], M. Pitt[175], L. Plazak[146a], M.-A. Pleier[27], V. Pleskot[86], E. Plotnikova[68], D. Pluth[67], P. Podberezko[111], R. Poettgen[148a,148b], R. Poggi[123a,123b], L. Poggioli[119], D. Pohl[23], G. Polesello[123a], A. Poley[45], A. Policicchio[40a,40b], R. Polifka[32], A. Polini[22a], C.S. Pollard[56], V. Polychronakos[27], K. Pommès[32], D. Ponomarenko[100], L. Pontecorvo[134a], G.A. Popeneciu[28d], A. Poppleton[32], S. Pospisil[130], K. Potamianos[16], I.N. Potrap[68], C.J. Potter[30], G. Poulard[32], T. Poulsen[84], J. Poveda[32], M.E. Pozo Astigarraga[32], P. Pralavorio[88], A. Pranko[16], S. Prell[67], D. Price[87], M. Primavera[76a], S. Prince[90], N. Proklova[100], K. Prokofiev[62c], F. Prokoshin[34b], S. Protopopescu[27], J. Proudfoot[6], M. Przybycien[41a], A. Puri[169], P. Puzo[119], J. Qian[92], G. Qin[56], Y. Qin[87], A. Quadt[57], M. Queitsch-Maitland[45], D. Quilty[56], S. Raddum[121], V. Radeka[27], V. Radescu[122], S.K. Radhakrishnan[150], P. Radloff[118], P. Rados[91], F. Ragusa[94a,94b], G. Rahal[181], J.A. Raine[87], S. Rajagopalan[27], C. Rangel-Smith[168], T. Rashid[119], S. Raspopov[5], M.G. Ratti[94a,94b], D.M. Rauch[45], F. Rauscher[102], S. Rave[86], I. Ravinovich[175], J.H. Rawling[87], M. Raymond[32], A.L. Read[121], N.P. Readioff[58], M. Reale[76a,76b], D.M. Rebuzzi[123a,123b], A. Redelbach[177], G. Redlinger[27], R. Reece[139], R.G. Reed[147c], K. Reeves[44], L. Rehnisch[17], J. Reichert[124], A. Reiss[86], C. Rembser[32], H. Ren[35a], M. Rescigno[134a], S. Resconi[94a], E.D. Resseguie[124], S. Rettie[171], E. Reynolds[19], O.L. Rezanova[111,c], P. Reznicek[131], R. Rezvani[97], R. Richter[103], S. Richter[81], E. Richter-Was[41b], O. Ricken[23], M. Ridel[83], P. Rieck[103], C.J. Riegel[178], J. Rieger[57], O. Rifki[115], M. Rijssenbeek[150], A. Rimoldi[123a,123b], M. Rimoldi[18], L. Rinaldi[22a], G. Ripellino[149], B. Ristić[32], E. Ritsch[32], I. Riu[13], F. Rizatdinova[116], E. Rizvi[79], C. Rizzi[13], R.T. Roberts[87], S.H. Robertson[90,o], A. Robichaud-Veronneau[90], D. Robinson[30], J.E.M. Robinson[45], A. Robson[56], E. Rocco[86], C. Roda[126a,126b], Y. Rodina[88,an], S. Rodriguez Bosca[170], A. Rodriguez Perez[13], D. Rodriguez Rodriguez[170], S. Roe[32], C.S. Rogan[59], O. Røhne[121], J. Roloff[59], A. Romaniouk[100], M. Romano[22a,22b], S.M. Romano Saez[37], E. Romero Adam[170], N. Rompotis[77], M. Ronzani[51], L. Roos[83], S. Rosati[134a], K. Rosbach[51], P. Rose[139], N.-A. Rosien[57], E. Rossi[106a,106b], L.P. Rossi[53a], J.H.N. Rosten[30], R. Rosten[140], M. Rotaru[28b], J. Rothberg[140], D. Rousseau[119], A. Rozanov[88], Y. Rozen[154], X. Ruan[147c], F. Rubbo[145], F. Rühr[51], A. Ruiz-Martinez[31], Z. Rurikova[51], N.A. Rusakovich[68], H.L. Russell[90], J.P. Rutherfoord[7], N. Ruthmann[32], Y.F. Ryabov[125], M. Rybar[169], G. Rybkin[119], S. Ryu[6], A. Ryzhov[132], G.F. Rzehorz[57], A.F. Saavedra[152], G. Sabato[109], S. Sacerdoti[29], H.F-W. Sadrozinski[139], R. Sadykov[68], F. Safai Tehrani[134a], P. Saha[110], M. Sahinsoy[60a], M. Saimpert[45], M. Saito[157], T. Saito[157], H. Sakamoto[157], Y. Sakurai[174], G. Salamanna[136a,136b], J.E. Salazar Loyola[34b], D. Salek[109], P.H. Sales De Bruin[168], D. Salihagic[103], A. Salnikov[145], J. Salt[170], D. Salvatore[40a,40b], F. Salvatore[151], A. Salvucci[62a,62b,62c], A. Salzburger[32], D. Sammel[51], D. Sampsonidis[156], D. Sampsonidou[156], J. Sánchez[170], V. Sanchez Martinez[170], A. Sanchez Pineda[167a,167c], H. Sandaker[121], R.L. Sandbach[79], C.O. Sander[45], M. Sandhoff[178],

JHEP11(2017)086

C. Sandoval[21], D.P.C. Sankey[133], M. Sannino[53a,53b], Y. Sano[105], A. Sansoni[50], C. Santoni[37], H. Santos[128a], I. Santoyo Castillo[151], A. Sapronov[68], J.G. Saraiva[128a,128d], B. Sarrazin[23], O. Sasaki[69], K. Sato[164], E. Sauvan[5], G. Savage[80], P. Savard[161,d], N. Savic[103], C. Sawyer[133], L. Sawyer[82,u], J. Saxon[33], C. Sbarra[22a], A. Sbrizzi[22a,22b], T. Scanlon[81], D.A. Scannicchio[166], M. Scarcella[152], J. Schaarschmidt[140], P. Schacht[103], B.M. Schachtner[102], D. Schaefer[32], L. Schaefer[124], R. Schaefer[45], J. Schaeffer[86], S. Schaepe[23], S. Schaetzel[60b], U. Schäfer[86], A.C. Schaffer[119], D. Schaile[102], R.D. Schamberger[150], V.A. Schegelsky[125], D. Scheirich[131], M. Schernau[166], C. Schiavi[53a,53b], S. Schier[139], L.K. Schildgen[23], C. Schillo[51], M. Schioppa[40a,40b], S. Schlenker[32], K.R. Schmidt-Sommerfeld[103], K. Schmieden[32], C. Schmitt[86], S. Schmitt[45], S. Schmitz[86], U. Schnoor[51], L. Schoeffel[138], A. Schoening[60b], B.D. Schoenrock[93], E. Schopf[23], M. Schott[86], J.F.P. Schouwenberg[108], J. Schovancova[32], S. Schramm[52], N. Schuh[86], A. Schulte[86], M.J. Schultens[23], H.-C. Schultz-Coulon[60a], H. Schulz[17], M. Schumacher[51], B.A. Schumm[139], Ph. Schune[138], A. Schwartzman[145], T.A. Schwarz[92], H. Schweiger[87], Ph. Schwemling[138], R. Schwienhorst[93], J. Schwindling[138], A. Sciandra[23], G. Sciolla[25], M. Scornajenghi[40a,40b], F. Scuri[126a,126b], F. Scutti[91], J. Searcy[92], P. Seema[23], S.C. Seidel[107], A. Seiden[139], J.M. Seixas[26a], G. Sekhniaidze[106a], K. Sekhon[92], S.J. Sekula[43], N. Semprini-Cesari[22a,22b], S. Senkin[37], C. Serfon[121], L. Serin[119], L. Serkin[167a,167b], M. Sessa[136a,136b], R. Seuster[172], H. Severini[115], T. Sfiligoj[78], F. Sforza[32], A. Sfyrla[52], E. Shabalina[57], N.W. Shaikh[148a,148b], L.Y. Shan[35a], R. Shang[169], J.T. Shank[24], M. Shapiro[16], P.B. Shatalov[99], K. Shaw[167a,167b], S.M. Shaw[87], A. Shcherbakova[148a,148b], C.Y. Shehu[151], Y. Shen[115], N. Sherafati[31], P. Sherwood[81], L. Shi[153,ao], S. Shimizu[70], C.O. Shimmin[179], M. Shimojima[104], I.P.J. Shipsey[122], S. Shirabe[73], M. Shiyakova[68,ap], J. Shlomi[175], A. Shmeleva[98], D. Shoaleh Saadi[97], M.J. Shochet[33], S. Shojaii[94a], D.R. Shope[115], S. Shrestha[113], E. Shulga[100], M.A. Shupe[7], P. Sicho[129], A.M. Sickles[169], P.E. Sidebo[149], E. Sideras Haddad[147c], O. Sidiropoulou[177], A. Sidoti[22a,22b], F. Siegert[47], Dj. Sijacki[14], J. Silva[128a,128d], S.B. Silverstein[148a], V. Simak[130], Lj. Simic[14], S. Simion[119], E. Simioni[86], B. Simmons[81], M. Simon[86], P. Sinervo[161], N.B. Sinev[118], M. Sioli[22a,22b], G. Siragusa[177], I. Siral[92], S.Yu. Sivoklokov[101], J. Sjölin[148a,148b], M.B. Skinner[75], P. Skubic[115], M. Slater[19], T. Slavicek[130], M. Slawinska[42], K. Sliwa[165], R. Slovak[131], V. Smakhtin[175], B.H. Smart[5], J. Smiesko[146a], N. Smirnov[100], S.Yu. Smirnov[100], Y. Smirnov[100], L.N. Smirnova[101,aq], O. Smirnova[84], J.W. Smith[57], M.N.K. Smith[38], R.W. Smith[38], M. Smizanska[75], K. Smolek[130], A.A. Snesarev[98], I.M. Snyder[118], S. Snyder[27], R. Sobie[172,o], F. Socher[47], A. Soffer[155], A. Søgaard[49], D.A. Soh[153], G. Sokhrannyi[78], C.A. Solans Sanchez[32], M. Solar[130], E.Yu. Soldatov[100], U. Soldevila[170], A.A. Solodkov[132], A. Soloshenko[68], O.V. Solovyanov[132], V. Solovyev[125], P. Sommer[51], H. Son[165], A. Sopczak[130], D. Sosa[60b], C.L. Sotiropoulou[126a,126b], R. Soualah[167a,167c], A.M. Soukharev[111,c], D. South[45], B.C. Sowden[80], S. Spagnolo[76a,76b], M. Spalla[126a,126b], M. Spangenberg[173], F. Spanò[80], D. Sperlich[17], F. Spettel[103], T.M. Spieker[60a], R. Spighi[22a], G. Spigo[32], L.A. Spiller[91], M. Spousta[131], R.D. St. Denis[56,*], A. Stabile[94a], R. Stamen[60a], S. Stamm[17], E. Stanecka[42], R.W. Stanek[6], C. Stanescu[136a], M.M. Stanitzki[45], B.S. Stapf[109], S. Stapnes[121], E.A. Starchenko[132], G.H. Stark[33], J. Stark[58], S.H Stark[39], P. Staroba[129], P. Starovoitov[60a], S. Stärz[32], R. Staszewski[42], P. Steinberg[27], B. Stelzer[144], H.J. Stelzer[32], O. Stelzer-Chilton[163a], H. Stenzel[55], G.A. Stewart[56], M.C. Stockton[118], M. Stoebe[90], G. Stoicea[28b], P. Stolte[57], S. Stonjek[103], A.R. Stradling[8], A. Straessner[47], M.E. Stramaglia[18], J. Strandberg[149], S. Strandberg[148a,148b], M. Strauss[115], P. Strizenec[146b], R. Ströhmer[177], D.M. Strom[118], R. Stroynowski[43], A. Strubig[49], S.A. Stucci[27], B. Stugu[15], N.A. Styles[45], D. Su[145], J. Su[127], S. Suchek[60a], Y. Sugaya[120], M. Suk[130], V.V. Sulin[98], DMS Sultan[162a,162b], S. Sultansoy[4c], T. Sumida[71], S. Sun[59], X. Sun[3], K. Suruliz[151], C.J.E. Suster[152], M.R. Sutton[151], S. Suzuki[69], M. Svatos[129], M. Swiatlowski[33], S.P. Swift[2], I. Sykora[146a], T. Sykora[131], D. Ta[51], K. Tackmann[45], J. Taenzer[155], A. Taffard[166],

JHEP11(2017)086

R. Tafirout[163a], N. Taiblum[155], H. Takai[27], R. Takashima[72], E.H. Takasugi[103], T. Takeshita[142], Y. Takubo[69], M. Talby[88], A.A. Talyshev[111,c], J. Tanaka[157], M. Tanaka[159], R. Tanaka[119], S. Tanaka[69], R. Tanioka[70], B.B. Tannenwald[113], S. Tapia Araya[34b], S. Tapprogge[86], S. Tarem[154], G.F. Tartarelli[94a], P. Tas[131], M. Tasevsky[129], T. Tashiro[71], E. Tassi[40a,40b], A. Tavares Delgado[128a,128b], Y. Tayalati[137e], A.C. Taylor[107], G.N. Taylor[91], P.T.E. Taylor[91], W. Taylor[163b], P. Teixeira-Dias[80], D. Temple[144], H. Ten Kate[32], P.K. Teng[153], J.J. Teoh[120], F. Tepel[178], S. Terada[69], K. Terashi[157], J. Terron[85], S. Terzo[13], M. Testa[50], R.J. Teuscher[161,o], T. Theveneaux-Pelzer[88], F. Thiele[39], J.P. Thomas[19], J. Thomas-Wilsker[80], P.D. Thompson[19], A.S. Thompson[56], L.A. Thomsen[179], E. Thomson[124], M.J. Tibbetts[16], R.E. Ticse Torres[88], V.O. Tikhomirov[98,ar], Yu.A. Tikhonov[111,c], S. Timoshenko[100], P. Tipton[179], S. Tisserant[88], K. Todome[159], S. Todorova-Nova[5], S. Todt[47], J. Tojo[73], S. Tokár[146a], K. Tokushuku[69], E. Tolley[59], L. Tomlinson[87], M. Tomoto[105], L. Tompkins[145,as], K. Toms[107], B. Tong[59], P. Tornambe[51], E. Torrence[118], H. Torres[144], E. Torró Pastor[140], J. Toth[88,at], F. Touchard[88], D.R. Tovey[141], C.J. Treado[112], T. Trefzger[177], F. Tresoldi[151], A. Tricoli[27], I.M. Trigger[163a], S. Trincaz-Duvoid[83], M.F. Tripiana[13], W. Trischuk[161], B. Trocmé[58], A. Trofymov[45], C. Troncon[94a], M. Trottier-McDonald[16], M. Trovatelli[172], L. Truong[147b], M. Trzebinski[42], A. Trzupek[42], K.W. Tsang[62a], J.C-L. Tseng[122], P.V. Tsiareshka[95], G. Tsipolitis[10], N. Tsirintanis[9], S. Tsiskaridze[13], V. Tsiskaridze[51], E.G. Tskhadadze[54a], K.M. Tsui[62a], I.I. Tsukerman[99], V. Tsulaia[16], S. Tsuno[69], D. Tsybychev[150], Y. Tu[62b], A. Tudorache[28b], V. Tudorache[28b], T.T. Tulbure[28a], A.N. Tuna[59], S.A. Tupputi[22a,22b], S. Turchikhin[68], D. Turgeman[175], I. Turk Cakir[4b,au], R. Turra[94a], P.M. Tuts[38], G. Ucchielli[22a,22b], I. Ueda[69], M. Ughetto[148a,148b], F. Ukegawa[164], G. Unal[32], A. Undrus[27], G. Unel[166], F.C. Ungaro[91], Y. Unno[69], C. Unverdorben[102], J. Urban[146b], P. Urquijo[91], P. Urrejola[86], G. Usai[8], J. Usui[69], L. Vacavant[88], V. Vacek[130], B. Vachon[90], K.O.H. Vadla[121], A. Vaidya[81], C. Valderanis[102], E. Valdes Santurio[148a,148b], S. Valentinetti[22a,22b], A. Valero[170], L. Valéry[13], S. Valkar[131], A. Vallier[5], J.A. Valls Ferrer[170], W. Van Den Wollenberg[109], H. van der Graaf[109], P. van Gemmeren[6], J. Van Nieuwkoop[144], I. van Vulpen[109], M.C. van Woerden[109], M. Vanadia[135a,135b], W. Vandelli[32], A. Vaniachine[160], P. Vankov[109], G. Vardanyan[180], R. Vari[134a], E.W. Varnes[7], C. Varni[53a,53b], T. Varol[43], D. Varouchas[119], A. Vartapetian[8], K.E. Varvell[152], J.G. Vasquez[179], G.A. Vasquez[34b], F. Vazeille[37], T. Vazquez Schroeder[90], J. Veatch[57], V. Veeraraghavan[7], L.M. Veloce[161], F. Veloso[128a,128c], S. Veneziano[134a], A. Ventura[76a,76b], M. Venturi[172], N. Venturi[32], A. Venturini[25], V. Vercesi[123a], M. Verducci[136a,136b], W. Verkerke[109], A.T. Vermeulen[109], J.C. Vermeulen[109], M.C. Vetterli[144,d], N. Viaux Maira[34b], O. Viazlo[84], I. Vichou[169,*], T. Vickey[141], O.E. Vickey Boeriu[141], G.H.A. Viehhauser[122], S. Viel[16], L. Vigani[122], M. Villa[22a,22b], M. Villaplana Perez[94a,94b], E. Vilucchi[50], M.G. Vincter[31], V.B. Vinogradov[68], A. Vishwakarma[45], C. Vittori[22a,22b], I. Vivarelli[151], S. Vlachos[10], M. Vogel[178], P. Vokac[130], G. Volpi[126a,126b], H. von der Schmitt[103], E. von Toerne[23], V. Vorobel[131], K. Vorobev[100], M. Vos[170], R. Voss[32], J.H. Vossebeld[77], N. Vranjes[14], M. Vranjes Milosavljevic[14], V. Vrba[130], M. Vreeswijk[109], R. Vuillermet[32], I. Vukotic[33], P. Wagner[23], W. Wagner[178], J. Wagner-Kuhr[102], H. Wahlberg[74], S. Wahrmund[47], J. Wakabayashi[105], J. Walder[75], R. Walker[102], W. Walkowiak[143], V. Wallangen[148a,148b], C. Wang[35b], C. Wang[36b,av], F. Wang[176], H. Wang[16], H. Wang[3], J. Wang[45], J. Wang[152], Q. Wang[115], R. Wang[6], S.M. Wang[153], T. Wang[38], W. Wang[153,aw], W. Wang[36a], Z. Wang[36c], C. Wanotayaroj[118], A. Warburton[90], C.P. Ward[30], D.R. Wardrope[81], A. Washbrook[49], P.M. Watkins[19], A.T. Watson[19], M.F. Watson[19], G. Watts[140], S. Watts[87], B.M. Waugh[81], A.F. Webb[11], S. Webb[86], M.S. Weber[18], S.W. Weber[177], S.A. Weber[31], J.S. Webster[6], A.R. Weidberg[122], B. Weinert[64], J. Weingarten[57], M. Weirich[86], C. Weiser[51], H. Weits[109], P.S. Wells[32], T. Wenaus[27], T. Wengler[32], S. Wenig[32], N. Wermes[23], M.D. Werner[67], P. Werner[32], M. Wessels[60a], K. Whalen[118], N.L. Whallon[140], A.M. Wharton[75], A.S. White[92],

JHEP11(2017)086

A. White[8], M.J. White[1], R. White[34b], D. Whiteson[166], B.W. Whitmore[75], F.J. Wickens[133], W. Wiedenmann[176], M. Wielers[133], C. Wiglesworth[39], L.A.M. Wiik-Fuchs[51], A. Wildauer[103], F. Wilk[87], H.G. Wilkens[32], H.H. Williams[124], S. Williams[109], C. Willis[93], S. Willocq[89], J.A. Wilson[19], I. Wingerter-Seez[5], E. Winkels[151], F. Winklmeier[118], O.J. Winston[151], B.T. Winter[23], M. Wittgen[145], M. Wobisch[82,u], T.M.H. Wolf[109], R. Wolff[88], M.W. Wolter[42], H. Wolters[128a,128c], V.W.S. Wong[171], S.D. Worm[19], B.K. Wosiek[42], J. Wotschack[32], K.W. Wozniak[42], M. Wu[33], S.L. Wu[176], X. Wu[52], Y. Wu[92], T.R. Wyatt[87], B.M. Wynne[49], S. Xella[39], Z. Xi[92], L. Xia[35c], D. Xu[35a], L. Xu[27], T. Xu[138], B. Yabsley[152], S. Yacoob[147a], D. Yamaguchi[159], Y. Yamaguchi[120], A. Yamamoto[69], S. Yamamoto[157], T. Yamanaka[157], M. Yamatani[157], K. Yamauchi[105], Y. Yamazaki[70], Z. Yan[24], H. Yang[36c], H. Yang[16], Y. Yang[153], Z. Yang[15], W-M. Yao[16], Y.C. Yap[83], Y. Yasu[69], E. Yatsenko[5], K.H. Yau Wong[23], J. Ye[43], S. Ye[27], I. Yeletskikh[68], E. Yigitbasi[24], E. Yildirim[86], K. Yorita[174], K. Yoshihara[124], C. Young[145], C.J.S. Young[32], J. Yu[8], J. Yu[67], S.P.Y. Yuen[23], I. Yusuff[30,ax], B. Zabinski[42], G. Zacharis[10], R. Zaidan[13], A.M. Zaitsev[132,al], N. Zakharchuk[45], J. Zalieckas[15], A. Zaman[150], S. Zambito[59], D. Zanzi[91], C. Zeitnitz[178], G. Zemaityte[122], A. Zemla[41a], J.C. Zeng[169], Q. Zeng[145], O. Zenin[132], T. Ženiš[146a], D. Zerwas[119], D. Zhang[92], F. Zhang[176], G. Zhang[36a,ay], H. Zhang[35b], J. Zhang[6], L. Zhang[51], L. Zhang[36a], M. Zhang[169], P. Zhang[35b], R. Zhang[23], R. Zhang[36a,av], X. Zhang[36b], Y. Zhang[35a], Z. Zhang[119], X. Zhao[43], Y. Zhao[36b,az], Z. Zhao[36a], A. Zhemchugov[68], B. Zhou[92], C. Zhou[176], L. Zhou[43], M. Zhou[35a], M. Zhou[150], N. Zhou[35c], C.G. Zhu[36b], H. Zhu[35a], J. Zhu[92], Y. Zhu[36a], X. Zhuang[35a], K. Zhukov[98], A. Zibell[177], D. Zieminska[64], N.I. Zimine[68], C. Zimmermann[86], S. Zimmermann[51], Z. Zinonos[103], M. Zinser[86], M. Ziolkowski[143], L. Živković[14], G. Zobernig[176], A. Zoccoli[22a,22b], R. Zou[33], M. zur Nedden[17], L. Zwalinski[32].

[1] *Department of Physics, University of Adelaide, Adelaide, Australia*
[2] *Physics Department, SUNY Albany, Albany NY, United States of America*
[3] *Department of Physics, University of Alberta, Edmonton AB, Canada*
[4] [(a)] *Department of Physics, Ankara University, Ankara;* [(b)] *Istanbul Aydin University, Istanbul;* [(c)] *Division of Physics, TOBB University of Economics and Technology, Ankara, Turkey*
[5] *LAPP, CNRS/IN2P3 and Université Savoie Mont Blanc, Annecy-le-Vieux, France*
[6] *High Energy Physics Division, Argonne National Laboratory, Argonne IL, United States of America*
[7] *Department of Physics, University of Arizona, Tucson AZ, United States of America*
[8] *Department of Physics, The University of Texas at Arlington, Arlington TX, United States of America*
[9] *Physics Department, National and Kapodistrian University of Athens, Athens, Greece*
[10] *Physics Department, National Technical University of Athens, Zografou, Greece*
[11] *Department of Physics, The University of Texas at Austin, Austin TX, United States of America*
[12] *Institute of Physics, Azerbaijan Academy of Sciences, Baku, Azerbaijan*
[13] *Institut de Física d'Altes Energies (IFAE), The Barcelona Institute of Science and Technology, Barcelona, Spain*
[14] *Institute of Physics, University of Belgrade, Belgrade, Serbia*
[15] *Department for Physics and Technology, University of Bergen, Bergen, Norway*
[16] *Physics Division, Lawrence Berkeley National Laboratory and University of California, Berkeley CA, United States of America*
[17] *Department of Physics, Humboldt University, Berlin, Germany*
[18] *Albert Einstein Center for Fundamental Physics and Laboratory for High Energy Physics, University of Bern, Bern, Switzerland*
[19] *School of Physics and Astronomy, University of Birmingham, Birmingham, United Kingdom*
[20] [(a)] *Department of Physics, Bogazici University, Istanbul;* [(b)] *Department of Physics Engineering, Gaziantep University, Gaziantep;* [(d)] *Istanbul Bilgi University, Faculty of Engineering and Natural Sciences, Istanbul;* [(e)] *Bahcesehir University, Faculty of Engineering and Natural Sciences, Istanbul, Turkey*

JHEP11(2017)086

[21] Centro de Investigaciones, Universidad Antonio Narino, Bogota, Colombia
[22] [(a)] INFN Sezione di Bologna; [(b)] Dipartimento di Fisica e Astronomia, Università di Bologna, Bologna, Italy
[23] Physikalisches Institut, University of Bonn, Bonn, Germany
[24] Department of Physics, Boston University, Boston MA, United States of America
[25] Department of Physics, Brandeis University, Waltham MA, United States of America
[26] [(a)] Universidade Federal do Rio De Janeiro COPPE/EE/IF, Rio de Janeiro; [(b)] Electrical Circuits Department, Federal University of Juiz de Fora (UFJF), Juiz de Fora; [(c)] Federal University of Sao Joao del Rei (UFSJ), Sao Joao del Rei; [(d)] Instituto de Fisica, Universidade de Sao Paulo, Sao Paulo, Brazil
[27] Physics Department, Brookhaven National Laboratory, Upton NY, United States of America
[28] [(a)] Transilvania University of Brasov, Brasov; [(b)] Horia Hulubei National Institute of Physics and Nuclear Engineering, Bucharest; [(c)] Department of Physics, Alexandru Ioan Cuza University of Iasi, Iasi; [(d)] National Institute for Research and Development of Isotopic and Molecular Technologies, Physics Department, Cluj Napoca; [(e)] University Politehnica Bucharest, Bucharest; [(f)] West University in Timisoara, Timisoara, Romania
[29] Departamento de Física, Universidad de Buenos Aires, Buenos Aires, Argentina
[30] Cavendish Laboratory, University of Cambridge, Cambridge, United Kingdom
[31] Department of Physics, Carleton University, Ottawa ON, Canada
[32] CERN, Geneva, Switzerland
[33] Enrico Fermi Institute, University of Chicago, Chicago IL, United States of America
[34] [(a)] Departamento de Física, Pontificia Universidad Católica de Chile, Santiago; [(b)] Departamento de Física, Universidad Técnica Federico Santa María, Valparaíso, Chile
[35] [(a)] Institute of High Energy Physics, Chinese Academy of Sciences, Beijing; [(b)] Department of Physics, Nanjing University, Jiangsu; [(c)] Physics Department, Tsinghua University, Beijing 100084, China
[36] [(a)] Department of Modern Physics and State Key Laboratory of Particle Detection and Electronics, University of Science and Technology of China, Anhui; [(b)] School of Physics, Shandong University, Shandong; [(c)] Department of Physics and Astronomy, Key Laboratory for Particle Physics, Astrophysics and Cosmology, Ministry of Education; Shanghai Key Laboratory for Particle Physics and Cosmology, Shanghai Jiao Tong University, Shanghai(also at PKU-CHEP), China
[37] Université Clermont Auvergne, CNRS/IN2P3, LPC, Clermont-Ferrand, France
[38] Nevis Laboratory, Columbia University, Irvington NY, United States of America
[39] Niels Bohr Institute, University of Copenhagen, Kobenhavn, Denmark
[40] [(a)] INFN Gruppo Collegato di Cosenza, Laboratori Nazionali di Frascati; [(b)] Dipartimento di Fisica, Università della Calabria, Rende, Italy
[41] [(a)] AGH University of Science and Technology, Faculty of Physics and Applied Computer Science, Krakow; [(b)] Marian Smoluchowski Institute of Physics, Jagiellonian University, Krakow, Poland
[42] Institute of Nuclear Physics Polish Academy of Sciences, Krakow, Poland
[43] Physics Department, Southern Methodist University, Dallas TX, United States of America
[44] Physics Department, University of Texas at Dallas, Richardson TX, United States of America
[45] DESY, Hamburg and Zeuthen, Germany
[46] Lehrstuhl für Experimentelle Physik IV, Technische Universität Dortmund, Dortmund, Germany
[47] Institut für Kern- und Teilchenphysik, Technische Universität Dresden, Dresden, Germany
[48] Department of Physics, Duke University, Durham NC, United States of America
[49] SUPA - School of Physics and Astronomy, University of Edinburgh, Edinburgh, United Kingdom
[50] INFN e Laboratori Nazionali di Frascati, Frascati, Italy
[51] Fakultät für Mathematik und Physik, Albert-Ludwigs-Universität, Freiburg, Germany
[52] Departement de Physique Nucleaire et Corpusculaire, Université de Genève, Geneva, Switzerland
[53] [(a)] INFN Sezione di Genova; [(b)] Dipartimento di Fisica, Università di Genova, Genova, Italy
[54] [(a)] E. Andronikashvili Institute of Physics, Iv. Javakhishvili Tbilisi State University, Tbilisi; [(b)] High Energy Physics Institute, Tbilisi State University, Tbilisi, Georgia

JHEP11(2017)086

[55] *II Physikalisches Institut, Justus-Liebig-Universität Giessen, Giessen, Germany*
[56] *SUPA - School of Physics and Astronomy, University of Glasgow, Glasgow, United Kingdom*
[57] *II Physikalisches Institut, Georg-August-Universität, Göttingen, Germany*
[58] *Laboratoire de Physique Subatomique et de Cosmologie, Université Grenoble-Alpes, CNRS/IN2P3, Grenoble, France*
[59] *Laboratory for Particle Physics and Cosmology, Harvard University, Cambridge MA, United States of America*
[60] [(a)] *Kirchhoff-Institut für Physik, Ruprecht-Karls-Universität Heidelberg, Heidelberg;* [(b)] *Physikalisches Institut, Ruprecht-Karls-Universität Heidelberg, Heidelberg, Germany*
[61] *Faculty of Applied Information Science, Hiroshima Institute of Technology, Hiroshima, Japan*
[62] [(a)] *Department of Physics, The Chinese University of Hong Kong, Shatin, N.T., Hong Kong;* [(b)] *Department of Physics, The University of Hong Kong, Hong Kong;* [(c)] *Department of Physics and Institute for Advanced Study, The Hong Kong University of Science and Technology, Clear Water Bay, Kowloon, Hong Kong, China*
[63] *Department of Physics, National Tsing Hua University, Taiwan, Taiwan*
[64] *Department of Physics, Indiana University, Bloomington IN, United States of America*
[65] *Institut für Astro- und Teilchenphysik, Leopold-Franzens-Universität, Innsbruck, Austria*
[66] *University of Iowa, Iowa City IA, United States of America*
[67] *Department of Physics and Astronomy, Iowa State University, Ames IA, United States of America*
[68] *Joint Institute for Nuclear Research, JINR Dubna, Dubna, Russia*
[69] *KEK, High Energy Accelerator Research Organization, Tsukuba, Japan*
[70] *Graduate School of Science, Kobe University, Kobe, Japan*
[71] *Faculty of Science, Kyoto University, Kyoto, Japan*
[72] *Kyoto University of Education, Kyoto, Japan*
[73] *Research Center for Advanced Particle Physics and Department of Physics, Kyushu University, Fukuoka, Japan*
[74] *Instituto de Física La Plata, Universidad Nacional de La Plata and CONICET, La Plata, Argentina*
[75] *Physics Department, Lancaster University, Lancaster, United Kingdom*
[76] [(a)] *INFN Sezione di Lecce;* [(b)] *Dipartimento di Matematica e Fisica, Università del Salento, Lecce, Italy*
[77] *Oliver Lodge Laboratory, University of Liverpool, Liverpool, United Kingdom*
[78] *Department of Experimental Particle Physics, Jožef Stefan Institute and Department of Physics, University of Ljubljana, Ljubljana, Slovenia*
[79] *School of Physics and Astronomy, Queen Mary University of London, London, United Kingdom*
[80] *Department of Physics, Royal Holloway University of London, Surrey, United Kingdom*
[81] *Department of Physics and Astronomy, University College London, London, United Kingdom*
[82] *Louisiana Tech University, Ruston LA, United States of America*
[83] *Laboratoire de Physique Nucléaire et de Hautes Energies, UPMC and Université Paris-Diderot and CNRS/IN2P3, Paris, France*
[84] *Fysiska institutionen, Lunds universitet, Lund, Sweden*
[85] *Departamento de Fisica Teorica C-15, Universidad Autonoma de Madrid, Madrid, Spain*
[86] *Institut für Physik, Universität Mainz, Mainz, Germany*
[87] *School of Physics and Astronomy, University of Manchester, Manchester, United Kingdom*
[88] *CPPM, Aix-Marseille Université and CNRS/IN2P3, Marseille, France*
[89] *Department of Physics, University of Massachusetts, Amherst MA, United States of America*
[90] *Department of Physics, McGill University, Montreal QC, Canada*
[91] *School of Physics, University of Melbourne, Victoria, Australia*
[92] *Department of Physics, The University of Michigan, Ann Arbor MI, United States of America*
[93] *Department of Physics and Astronomy, Michigan State University, East Lansing MI, United States of America*
[94] [(a)] *INFN Sezione di Milano;* [(b)] *Dipartimento di Fisica, Università di Milano, Milano, Italy*

JHEP11(2017)086

[95] B.I. Stepanov Institute of Physics, National Academy of Sciences of Belarus, Minsk, Republic of Belarus
[96] Research Institute for Nuclear Problems of Byelorussian State University, Minsk, Republic of Belarus
[97] Group of Particle Physics, University of Montreal, Montreal QC, Canada
[98] P.N. Lebedev Physical Institute of the Russian Academy of Sciences, Moscow, Russia
[99] Institute for Theoretical and Experimental Physics (ITEP), Moscow, Russia
[100] National Research Nuclear University MEPhI, Moscow, Russia
[101] D.V. Skobeltsyn Institute of Nuclear Physics, M.V. Lomonosov Moscow State University, Moscow, Russia
[102] Fakultät für Physik, Ludwig-Maximilians-Universität München, München, Germany
[103] Max-Planck-Institut für Physik (Werner-Heisenberg-Institut), München, Germany
[104] Nagasaki Institute of Applied Science, Nagasaki, Japan
[105] Graduate School of Science and Kobayashi-Maskawa Institute, Nagoya University, Nagoya, Japan
[106] [(a)] INFN Sezione di Napoli; [(b)] Dipartimento di Fisica, Università di Napoli, Napoli, Italy
[107] Department of Physics and Astronomy, University of New Mexico, Albuquerque NM, United States of America
[108] Institute for Mathematics, Astrophysics and Particle Physics, Radboud University Nijmegen/Nikhef, Nijmegen, Netherlands
[109] Nikhef National Institute for Subatomic Physics and University of Amsterdam, Amsterdam, Netherlands
[110] Department of Physics, Northern Illinois University, DeKalb IL, United States of America
[111] Budker Institute of Nuclear Physics, SB RAS, Novosibirsk, Russia
[112] Department of Physics, New York University, New York NY, United States of America
[113] Ohio State University, Columbus OH, United States of America
[114] Faculty of Science, Okayama University, Okayama, Japan
[115] Homer L. Dodge Department of Physics and Astronomy, University of Oklahoma, Norman OK, United States of America
[116] Department of Physics, Oklahoma State University, Stillwater OK, United States of America
[117] Palacký University, RCPTM, Olomouc, Czech Republic
[118] Center for High Energy Physics, University of Oregon, Eugene OR, United States of America
[119] LAL, Univ. Paris-Sud, CNRS/IN2P3, Université Paris-Saclay, Orsay, France
[120] Graduate School of Science, Osaka University, Osaka, Japan
[121] Department of Physics, University of Oslo, Oslo, Norway
[122] Department of Physics, Oxford University, Oxford, United Kingdom
[123] [(a)] INFN Sezione di Pavia; [(b)] Dipartimento di Fisica, Università di Pavia, Pavia, Italy
[124] Department of Physics, University of Pennsylvania, Philadelphia PA, United States of America
[125] National Research Centre "Kurchatov Institute" B.P.Konstantinov Petersburg Nuclear Physics Institute, St. Petersburg, Russia
[126] [(a)] INFN Sezione di Pisa; [(b)] Dipartimento di Fisica E. Fermi, Università di Pisa, Pisa, Italy
[127] Department of Physics and Astronomy, University of Pittsburgh, Pittsburgh PA, United States of America
[128] [(a)] Laboratório de Instrumentação e Física Experimental de Partículas - LIP, Lisboa; [(b)] Faculdade de Ciências, Universidade de Lisboa, Lisboa; [(c)] Department of Physics, University of Coimbra, Coimbra; [(d)] Centro de Física Nuclear da Universidade de Lisboa, Lisboa; [(e)] Departamento de Fisica, Universidade do Minho, Braga; [(f)] Departamento de Fisica Teorica y del Cosmos and CAFPE, Universidad de Granada, Granada; [(g)] Dep Fisica and CEFITEC of Faculdade de Ciencias e Tecnologia, Universidade Nova de Lisboa, Caparica, Portugal
[129] Institute of Physics, Academy of Sciences of the Czech Republic, Praha, Czech Republic
[130] Czech Technical University in Prague, Praha, Czech Republic
[131] Charles University, Faculty of Mathematics and Physics, Prague, Czech Republic
[132] State Research Center Institute for High Energy Physics (Protvino), NRC KI, Russia

JHEP11(2017)086

[133] *Particle Physics Department, Rutherford Appleton Laboratory, Didcot, United Kingdom*
[134] [(a)] *INFN Sezione di Roma;* [(b)] *Dipartimento di Fisica, Sapienza Università di Roma, Roma, Italy*
[135] [(a)] *INFN Sezione di Roma Tor Vergata;* [(b)] *Dipartimento di Fisica, Università di Roma Tor Vergata, Roma, Italy*
[136] [(a)] *INFN Sezione di Roma Tre;* [(b)] *Dipartimento di Matematica e Fisica, Università Roma Tre, Roma, Italy*
[137] [(a)] *Faculté des Sciences Ain Chock, Réseau Universitaire de Physique des Hautes Energies - Université Hassan II, Casablanca;* [(b)] *Centre National de l'Energie des Sciences Techniques Nucleaires, Rabat;* [(c)] *Faculté des Sciences Semlalia, Université Cadi Ayyad, LPHEA-Marrakech;* [(d)] *Faculté des Sciences, Université Mohamed Premier and LPTPM, Oujda;* [(e)] *Faculté des sciences, Université Mohammed V, Rabat, Morocco*
[138] *DSM/IRFU (Institut de Recherches sur les Lois Fondamentales de l'Univers), CEA Saclay (Commissariat à l'Energie Atomique et aux Energies Alternatives), Gif-sur-Yvette, France*
[139] *Santa Cruz Institute for Particle Physics, University of California Santa Cruz, Santa Cruz CA, United States of America*
[140] *Department of Physics, University of Washington, Seattle WA, United States of America*
[141] *Department of Physics and Astronomy, University of Sheffield, Sheffield, United Kingdom*
[142] *Department of Physics, Shinshu University, Nagano, Japan*
[143] *Department Physik, Universität Siegen, Siegen, Germany*
[144] *Department of Physics, Simon Fraser University, Burnaby BC, Canada*
[145] *SLAC National Accelerator Laboratory, Stanford CA, United States of America*
[146] [(a)] *Faculty of Mathematics, Physics & Informatics, Comenius University, Bratislava;* [(b)] *Department of Subnuclear Physics, Institute of Experimental Physics of the Slovak Academy of Sciences, Kosice, Slovak Republic*
[147] [(a)] *Department of Physics, University of Cape Town, Cape Town;* [(b)] *Department of Physics, University of Johannesburg, Johannesburg;* [(c)] *School of Physics, University of the Witwatersrand, Johannesburg, South Africa*
[148] [(a)] *Department of Physics, Stockholm University;* [(b)] *The Oskar Klein Centre, Stockholm, Sweden*
[149] *Physics Department, Royal Institute of Technology, Stockholm, Sweden*
[150] *Departments of Physics & Astronomy and Chemistry, Stony Brook University, Stony Brook NY, United States of America*
[151] *Department of Physics and Astronomy, University of Sussex, Brighton, United Kingdom*
[152] *School of Physics, University of Sydney, Sydney, Australia*
[153] *Institute of Physics, Academia Sinica, Taipei, Taiwan*
[154] *Department of Physics, Technion: Israel Institute of Technology, Haifa, Israel*
[155] *Raymond and Beverly Sackler School of Physics and Astronomy, Tel Aviv University, Tel Aviv, Israel*
[156] *Department of Physics, Aristotle University of Thessaloniki, Thessaloniki, Greece*
[157] *International Center for Elementary Particle Physics and Department of Physics, The University of Tokyo, Tokyo, Japan*
[158] *Graduate School of Science and Technology, Tokyo Metropolitan University, Tokyo, Japan*
[159] *Department of Physics, Tokyo Institute of Technology, Tokyo, Japan*
[160] *Tomsk State University, Tomsk, Russia*
[161] *Department of Physics, University of Toronto, Toronto ON, Canada*
[162] [(a)] *INFN-TIFPA;* [(b)] *University of Trento, Trento, Italy*
[163] [(a)] *TRIUMF, Vancouver BC;* [(b)] *Department of Physics and Astronomy, York University, Toronto ON, Canada*
[164] *Faculty of Pure and Applied Sciences, and Center for Integrated Research in Fundamental Science and Engineering, University of Tsukuba, Tsukuba, Japan*
[165] *Department of Physics and Astronomy, Tufts University, Medford MA, United States of America*
[166] *Department of Physics and Astronomy, University of California Irvine, Irvine CA, United States of America*

JHEP11(2017)086

[167] [(a)] *INFN Gruppo Collegato di Udine, Sezione di Trieste, Udine;* [(b)] *ICTP, Trieste;* [(c)] *Dipartimento di Chimica, Fisica e Ambiente, Università di Udine, Udine, Italy*
[168] *Department of Physics and Astronomy, University of Uppsala, Uppsala, Sweden*
[169] *Department of Physics, University of Illinois, Urbana IL, United States of America*
[170] *Instituto de Fisica Corpuscular (IFIC), Centro Mixto Universidad de Valencia - CSIC, Spain*
[171] *Department of Physics, University of British Columbia, Vancouver BC, Canada*
[172] *Department of Physics and Astronomy, University of Victoria, Victoria BC, Canada*
[173] *Department of Physics, University of Warwick, Coventry, United Kingdom*
[174] *Waseda University, Tokyo, Japan*
[175] *Department of Particle Physics, The Weizmann Institute of Science, Rehovot, Israel*
[176] *Department of Physics, University of Wisconsin, Madison WI, United States of America*
[177] *Fakultät für Physik und Astronomie, Julius-Maximilians-Universität, Würzburg, Germany*
[178] *Fakultät für Mathematik und Naturwissenschaften, Fachgruppe Physik, Bergische Universität Wuppertal, Wuppertal, Germany*
[179] *Department of Physics, Yale University, New Haven CT, United States of America*
[180] *Yerevan Physics Institute, Yerevan, Armenia*
[181] *Centre de Calcul de l'Institut National de Physique Nucléaire et de Physique des Particules (IN2P3), Villeurbanne, France*
[182] *Academia Sinica Grid Computing, Institute of Physics, Academia Sinica, Taipei, Taiwan*
[a] *Also at Department of Physics, King's College London, London, United Kingdom*
[b] *Also at Institute of Physics, Azerbaijan Academy of Sciences, Baku, Azerbaijan*
[c] *Also at Novosibirsk State University, Novosibirsk, Russia*
[d] *Also at TRIUMF, Vancouver BC, Canada*
[e] *Also at Department of Physics & Astronomy, University of Louisville, Louisville, KY, United States of America*
[f] *Also at Physics Department, An-Najah National University, Nablus, Palestine*
[g] *Also at Department of Physics, California State University, Fresno CA, United States of America*
[h] *Also at Department of Physics, University of Fribourg, Fribourg, Switzerland*
[i] *Also at II Physikalisches Institut, Georg-August-Universität, Göttingen, Germany*
[j] *Also at Departament de Fisica de la Universitat Autonoma de Barcelona, Barcelona, Spain*
[k] *Also at Departamento de Fisica e Astronomia, Faculdade de Ciencias, Universidade do Porto, Portugal*
[l] *Also at Tomsk State University, Tomsk, Russia*
[m] *Also at The Collaborative Innovation Center of Quantum Matter (CICQM), Beijing, China*
[n] *Also at Universita di Napoli Parthenope, Napoli, Italy*
[o] *Also at Institute of Particle Physics (IPP), Canada*
[p] *Also at Horia Hulubei National Institute of Physics and Nuclear Engineering, Bucharest, Romania*
[q] *Also at Department of Physics, St. Petersburg State Polytechnical University, St. Petersburg, Russia*
[r] *Also at Borough of Manhattan Community College, City University of New York, New York City, United States of America*
[s] *Also at Department of Financial and Management Engineering, University of the Aegean, Chios, Greece*
[t] *Also at Centre for High Performance Computing, CSIR Campus, Rosebank, Cape Town, South Africa*
[u] *Also at Louisiana Tech University, Ruston LA, United States of America*
[v] *Also at Institucio Catalana de Recerca i Estudis Avancats, ICREA, Barcelona, Spain*
[w] *Also at Graduate School of Science, Osaka University, Osaka, Japan*
[x] *Also at Fakultät für Mathematik und Physik, Albert-Ludwigs-Universität, Freiburg, Germany*
[y] *Also at Institute for Mathematics, Astrophysics and Particle Physics, Radboud University Nijmegen/Nikhef, Nijmegen, Netherlands*

JHEP11(2017)086

[z] Also at Department of Physics, The University of Texas at Austin, Austin TX, United States of America
[aa] Also at Institute of Theoretical Physics, Ilia State University, Tbilisi, Georgia
[ab] Also at CERN, Geneva, Switzerland
[ac] Also at Georgian Technical University (GTU),Tbilisi, Georgia
[ad] Also at Ochadai Academic Production, Ochanomizu University, Tokyo, Japan
[ae] Also at Manhattan College, New York NY, United States of America
[af] Also at Departamento de Física, Pontificia Universidad Católica de Chile, Santiago, Chile
[ag] Also at Department of Physics, The University of Michigan, Ann Arbor MI, United States of America
[ah] Also at The City College of New York, New York NY, United States of America
[ai] Also at School of Physics, Shandong University, Shandong, China
[aj] Also at Departamento de Fisica Teorica y del Cosmos and CAFPE, Universidad de Granada, Granada, Portugal
[ak] Also at Department of Physics, California State University, Sacramento CA, United States of America
[al] Also at Moscow Institute of Physics and Technology State University, Dolgoprudny, Russia
[am] Also at Departement de Physique Nucleaire et Corpusculaire, Université de Genève, Geneva, Switzerland
[an] Also at Institut de Física d'Altes Energies (IFAE), The Barcelona Institute of Science and Technology, Barcelona, Spain
[ao] Also at School of Physics, Sun Yat-sen University, Guangzhou, China
[ap] Also at Institute for Nuclear Research and Nuclear Energy (INRNE) of the Bulgarian Academy of Sciences, Sofia, Bulgaria
[aq] Also at Faculty of Physics, M.V.Lomonosov Moscow State University, Moscow, Russia
[ar] Also at National Research Nuclear University MEPhI, Moscow, Russia
[as] Also at Department of Physics, Stanford University, Stanford CA, United States of America
[at] Also at Institute for Particle and Nuclear Physics, Wigner Research Centre for Physics, Budapest, Hungary
[au] Also at Giresun University, Faculty of Engineering, Turkey
[av] Also at CPPM, Aix-Marseille Université and CNRS/IN2P3, Marseille, France
[aw] Also at Department of Physics, Nanjing University, Jiangsu, China
[ax] Also at University of Malaya, Department of Physics, Kuala Lumpur, Malaysia
[ay] Also at Institute of Physics, Academia Sinica, Taipei, Taiwan
[az] Also at LAL, Univ. Paris-Sud, CNRS/IN2P3, Université Paris-Saclay, Orsay, France
[*] Deceased

JHEP11(2017)086